1989

The evolution of the Mishibishu greenstone belt, near Wawa, Ontario.

Richard John. Keller
University of Windsor

NOTICE

The quality of this microform is heavily dependent upon the quality of the original thesis submitted for microfilming. Every effort has been made to ensure the highest quality of reproduction possible.

If pages are missing, contact the university which granted the degree.

Some pages may have indistinct print especially if the original pages were typed with a poor typewriter ribbon or if the university sent us an inferior photocopy.

Reproduction in full or in part of this microform is governed by the Canadian Copyright Act, R.S.C. 1970, c. C-30, and subsequent amendments.

AVIS

La qualité de cette microforme dépend grandement de la qualité de la thèse soumise au microfilmage. Nous avons tout fait pour assurer une qualité supérieure de reproduction.

S'il manque des pages, veuillez communiquer avec l'université qui a conféré le grade.

La qualité d'impression de certaines pages peut laisser à désirer, surtout si les pages originales ont été dactylographiées à l'aide d'un ruban usé ou si l'université nous a fait parvenir une photocopie de qualité inférieure.

La reproduction, même partielle, de cette microforme est soumise à la Loi canadienne sur le droit d'auteur, SRC 1970, c. C-30, et ses amendements subséquents.

THE EVOLUTION OF THE MISHIBISHU GREENSTONE BELT, NEAR WAWA, ONTARIO

by

© Richard John Keller

A Thesis
Submitted to the
Faculty of Graduate Studies and Research
through the Department of Geology
in Partial Fulfillment of
the Requirements for the
Degree of Master of Science at
the University of Windsor

Windsor, Ontario, Canada

1989

ISBN 0-315-54536-4

ABSTRACT

The Mishibishu greenstone belt is located approximately 40 km west of Wawa, and is currently the focus of active gold mining and exploration. The belt trends east-west and it is probably an extension of the Michipicoten greenstone belt, although the two belts are physically separated by granitoid terrain. The mafic metavolcanic supracrustal rocks are Mg-Fe tholeiites, and grade into intermediate metavolcanics of calc-alkaline composition. Felsic metavolcanics are calc-alkaline in composition, and are not very extensive in the belt. Metasedimentary rocks are dominantly greywacke, siltstone, and argillite, while minor conglomerates, chert, and iron formation are also encountered. The supracrustal rocks are embayed and intruded by granitoid plutons of granitic, dioritic, and gabbroic composition.

U-Pb zircon ages were determined for seven rock units. The oldest rock is the Jostle Lake tonalite, with an age of 2721 ± 4 Ma, from the Northern Batholithic Complex. The Chimney Point subvolcanic quartz-feldspar porphyry has an age of 2696 ± 17 Ma, and the Pilot Harbour granite, from the Southern batholith, has a similar age of 2693 ± 7 Ma. A felsic pyroclastic breccia collected near David Lakes yields an age of 2677 ± 7 Ma. Plutonic rocks in this age range are the Tee Lake tonalite at 2673 ± 12 Ma, which is a pluton in

the Northern Batholithic Complex, and the Iron Lake gabbro, at 2671 ± 4 Ma, which intrudes both the Kabenung belt and the Northern Batholithic Complex north of the Mishibishu belt. The age of the Bowman Lake granite is an interpreted age of ca. 2672 Ma.

The ages in the Mishibishu belt are comparable to those reported for rocks in the Wawa and Gamitagama greenstone belts, except for the 2677 Ma age for the felsic pyroclastic rock, which is the first such age determined for an Archean volcanic rock in the Superior Province.

ACKNOWLEDGEMENTS

My sincere appreciation goes to my advisor, Dr. A. Turek, who contributed greatly to my knowledge over the duration of this research project. I also wish to thank R.G. Reid regarding the discussions of geology of the study area, and for the maps which he kindly provided. Thanks to W.R. Van Schmus for allowing me to use his laboratory facilities at the University of Kansas Isotope Geology Laboratory, and to B. Dobson, P. McMahon and I. Churchill for their assistance in mineral separation. My thanks also goes to W.D. Taylor and all the members of the mapping crews of the Ontario Geological Survey for their assistance in sample collection. This project was made possible through funding to A. Turek by the Ontario Geological Survey, and the Natural Sciences and Engineering Research Council of Canada.

TABLE OF CONTENTS

LIST OF TABLES

LIST OF FIGURES

LIST OF APPENDICES

CHAPTER I

INTRODUCTION

The Mishibishu Lake greenstone belt is located in the Wawa Subprovince of the Superior Province approximately 40 km west of Wawa, Ontario, on the shore of Lake Superior with approximate dimensions of 30 km width and 60 km length. The belt trends east-west, and is intruded by several granitoid plutons. The supracrustal rocks are embayed by granitoid terrain which also separates it from the Kabenung Lake belt to the north.

The first recorded mapping of the region was by Louis Agassiz in 1850, followed by Logan in 1863 (Bennett and Thurston 1977). Coleman (1899) and Coleman and Willmott (1899) summarized the distribution of greenstone belts and iron deposits in the area. A larger, more detailed survey by Bell (1905) included a portion of the Mishibishu area and the Wawa area. The region between Mishibishu Lake and the East Pukaskwa River was mapped by Evans (1940). The Kabenung Lake area to the north was mapped by Goodwin (1954). In 1968, reconnaissance mapping of the Pukaskwa River - University River area was done by Bennett and Thurston (1977), and a subsequent geochemical survey was performed by Wolfe (1976). A three-year reconnaissance mapping program, undertaken by the Ontario Geological

Survey, was carried out by Bowen and Logothetis (1985), Bowen (1986), and Reid and Reilly (1987). A final report for the area is in preparation by Reid et al. (1989).

Gold was first discovered in the vicinity in 1897 on the shore of Wawa Lake, and prospecting has been active since the 1930's. The recent discoveries of gold around Wawa and in the Hemlo area have created a renewed interest in the Mishibishu greenstone belt. A report summarizing the mineralization within the Mishibishu Lake area is given by Heather (1985, 1986).

No previous ages of any kind have been reported for the Mishibishu Lake greenstone belt. This study reports seven U-Pb zircon ages for volcanic and plutonic rocks, and thus provides precise timing of the various magmatic episodes and volcanic events in the evolution of the greenstone belt.

CHAPTER II

GEOLOGY

The geology of the Mishibishu greenstone belt given here follows that of Bennett and Thurston (1977) and Reid et al. (1989), because these are the most recent and comprehensive reports on the area. A simplified map of geology is shown in Figure 1, and Table 1 is a table of lithologic units after Bennett and Thurston (1977). The stratigraphy given in this table does not always follow that seen in the Mishibishu belt because it includes lithologic units from the Kabenung belt north of the study area.

The oldest rocks in the belt are mafic metavolcanics, which consist of massive to pillowed flows of basalt to andesite, and pyroclastics such as tuff, lapilli tuff, and breccia. The composition of these mafic rocks ranges from magnesium- and iron-tholeiites to calc-alkaline basalt and andesite. Porphyritic basalts are common with grain sizes large enough to warrant their classification as plutonic. These could represent sills and dikes, or they may be subvolcanic intrusions related to mafic volcanism. Mafic metavolcanics grade into intermediate metavolcanics of tholeiitic to calc-alkaline composition and include andesitic to dacitic flows with associated pyroclastic flows lapilli tuff, crystal tuff, and vitric tuff.

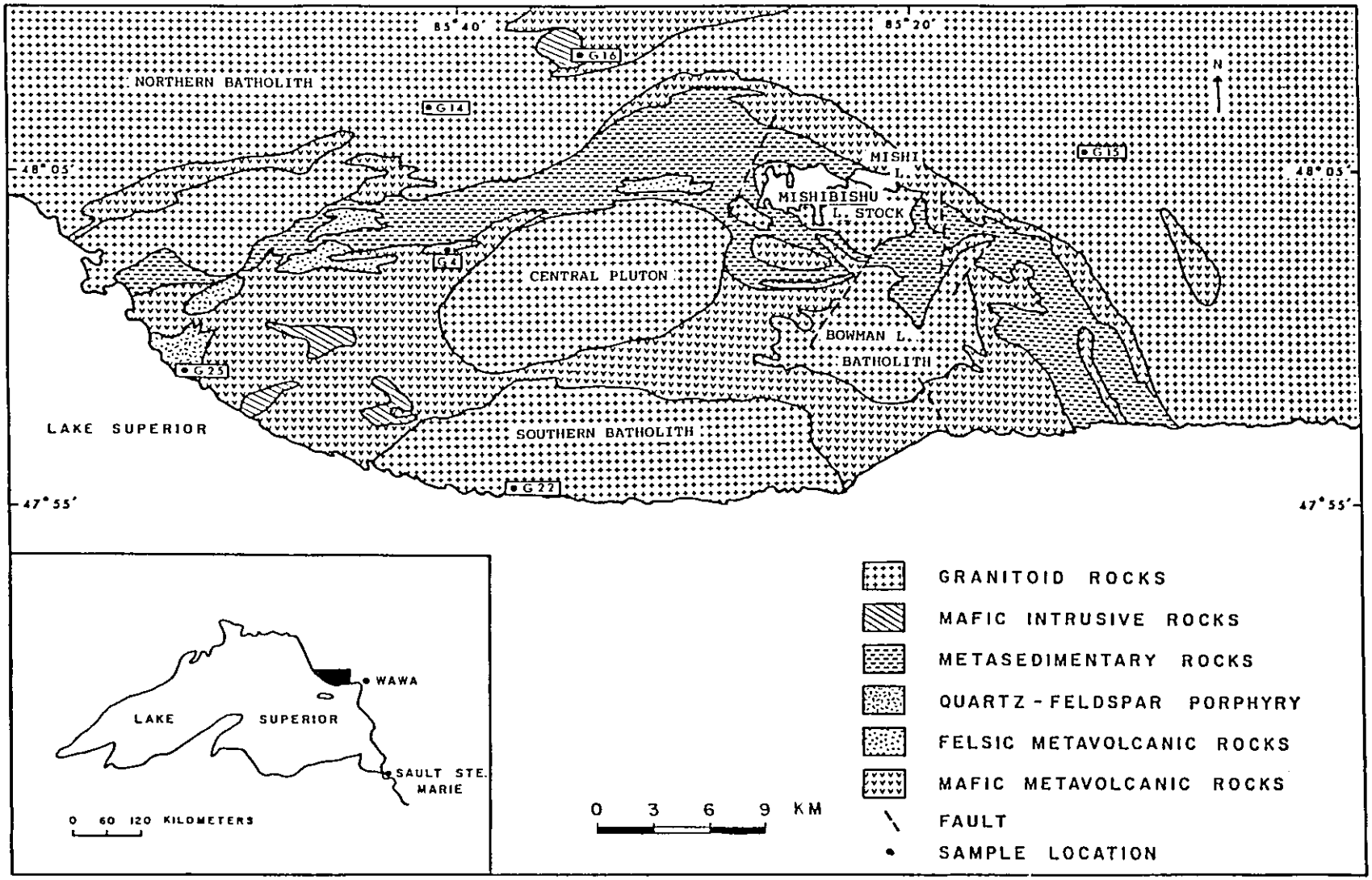

Figure 1. Simplified geological map of the Precambrian rocks of the Mishibishu greenstone belt, with sample locations (based on Reid et al., 1989).

Table 1. Precambrian lithologic units of the Mishibishu greenstone belt (after Bennett and Thurston 1977)

LATE MAFIC INTRUSIVE ROCKS

Diabase dikes, gabbro

FELSIC INTRUSIVE ROCKS

MISHIBISHU LAKE STOCK

Porphyritic monzonite, quartz monzonite

BATHOLITHIC GRANITIC ROCKS

Quartz monzonite, trondhjemite, granite, aplite, hornblende diorite-gneiss, biotite granite-gneiss

METASEDIMENTS

Greywacke, arkose, siltstone, argilite, conglomerate, iron formation

METAVOLCANICS

FELSIC TO INTERMEDIATE METAVOLCANICS

Dacite to rhyolite flows, felsic to intermediate tuff and volcanic breccia, quartz-feldspar porphyry

MAFIC TO INTERMEDIATE METAVOLCANICS AND RELATED INTRUSIVE ROCKS

Basalt, pillow basalt, porphyritic basalt, andesite, gabbro, porphyritic gabbro

IRON FORMATION

Felsic to intermediate metavolcanics of calc-alkaline composition are composed dominantly of pyroclastic units such as tuff, lapilli tuff, breccia, and porphyritic flows. Dacitic to rhyolitic flows are also found, but are sparsely distributed throughout the Mishibishu belt, and occur mostly in the western part of the belt, together with several units of subvolcanic quartz-feldspar porphyry, which may be related to the felsic volcanism.

An exhalative event appears to have capped this volcanic cycle with iron formation composed of alternating beds of chert or red jasper, and magnetite or hematite. All four facies of the Michipicoten-type iron formation have been identified in the Mishibishu area. The characteristics of these were set by Collins and Quirke (1926) as follows:

1. mafic metavolcanics form a cover over the iron formation
2. a sharp contact exists between mafic metavolcanics and underlying banded chert-magnetite iron
3. a sharp alternating contact between the chert-magnetite member from the underlying pyrite
4. pyrite member grades downward into a siderite member
5. siderite member grades downward into a felsic volcanic unit which forms the footwall of the iron formation.

These dominant oxide-facies formations may grade locally into carbonate facies (siderite). Minor amounts of a silicate-facies iron formation may be interbedded with the

oxide facies. Magnetite and quartz usually occur with the silicates. The MacLeod Mine in Wawa, is in the oxide-facies type of iron ore.

The clastic metasedimentary rocks in the area are probably derived from volcanic and granitic rocks from the area, but are mainly erosion products of the volcanic pile. The most common metasediments are greywacke and siltstone, and graded bedding is often encountered in these. Frequently, argillite and mudstone may be found at the top of graded beds of greywacke. Conglomerates are abundant and have a wide range in clast size and composition. Clasts are generally subrounded to well-rounded pebble to boulder-size, set in an arkosic wacke matrix. Clast composition may be anything from volcanic breccia to granitic cobbles and boulders. Goodwin (1962) concluded that the conglomerates in this region are alluvial fan deposits and that the granitic boulders were probably derived from subvolcanic granitic intrusions. This implies that there need not have been a pre-existing granitic terrain. This idea is supported by a study by Bass (1961), who concluded that granitic boulders in the Dore conglomerate in the Abitibi greenstone belt originated from subvolcanic stocks.

Felsic plugs, stocks, and batholiths intrude and embay the supracrustal rocks of the Mishibishu belt. Internal felsic intrusions include the Central Pluton, and the Mishibishu Lake stock, which are granitic and relatively

homogeneous in composition, and the Bowman Lake batholith, which is a compositionally variable porphyritic granite. The external granitic terrain is referred to as the Northern Batholithic Complex because of the numerous mappable granitoid intrusions that ccmprise it. The composition of these rocks ranges from diorite through tonalite, to granite. To the south of the belt and along the Lake Superior shoreline, is the Southern batholith, which is granitic in composition.

Internal mafic intrusions consist of several coarse-grained, small gabbroic plugs in the vicinity of Loon Lake in the western part of the area. These plugs are belieaved to be related to mafic volcanism during which synvolcanic dikes and sills were probably emplaced. Relevant to this study, but outside the Mishibishu belt, is the Iron Lake gabbro which intrudes the southwest end of the Kabenung greenstone belt and the Northern Batholithic Complex.

The structural trend of the Mishibishu Lake greenstone belt is approximately east-west. The rocks have been metamorphosed to greenschist facies, though in localized areas of the belt, the metamorphism extends to lower amphibolite facies.

The supracrustal rocks are folded into a steeply dipping isoclinal synformal structure. The Kink Lake Anticline is located in the southwestern part of the area and plunges shallowly to the northwest. A 28 km long

overturned syncline extends west, starting at Mishibishu Lake, through metasedimentary units near the northern boundary of the belt. A major shear zone, the Mishibishu Lake Deformation Zone (Fig. 2), trends subparallel to the strike of the metavolcanic-metasedimentary sequences, extending about 35 km from the southeast boundary of the belt to northwest of Mishibishu Lake, along the northern contact with the Northern Batholithic Complex. Current gold mining interests are focused in this area.

There are only two major faults, both of which are northeast-trending. One fault is located about 1 km west of Mishibishu Lake, and the other extends from the Bowman Lake batholith through Katzenbach Lake. Lateral displacements are approximately 6 and 10 km, respectively, and from field relations, both faults are believed to have occurred later than the granitic intrusions.

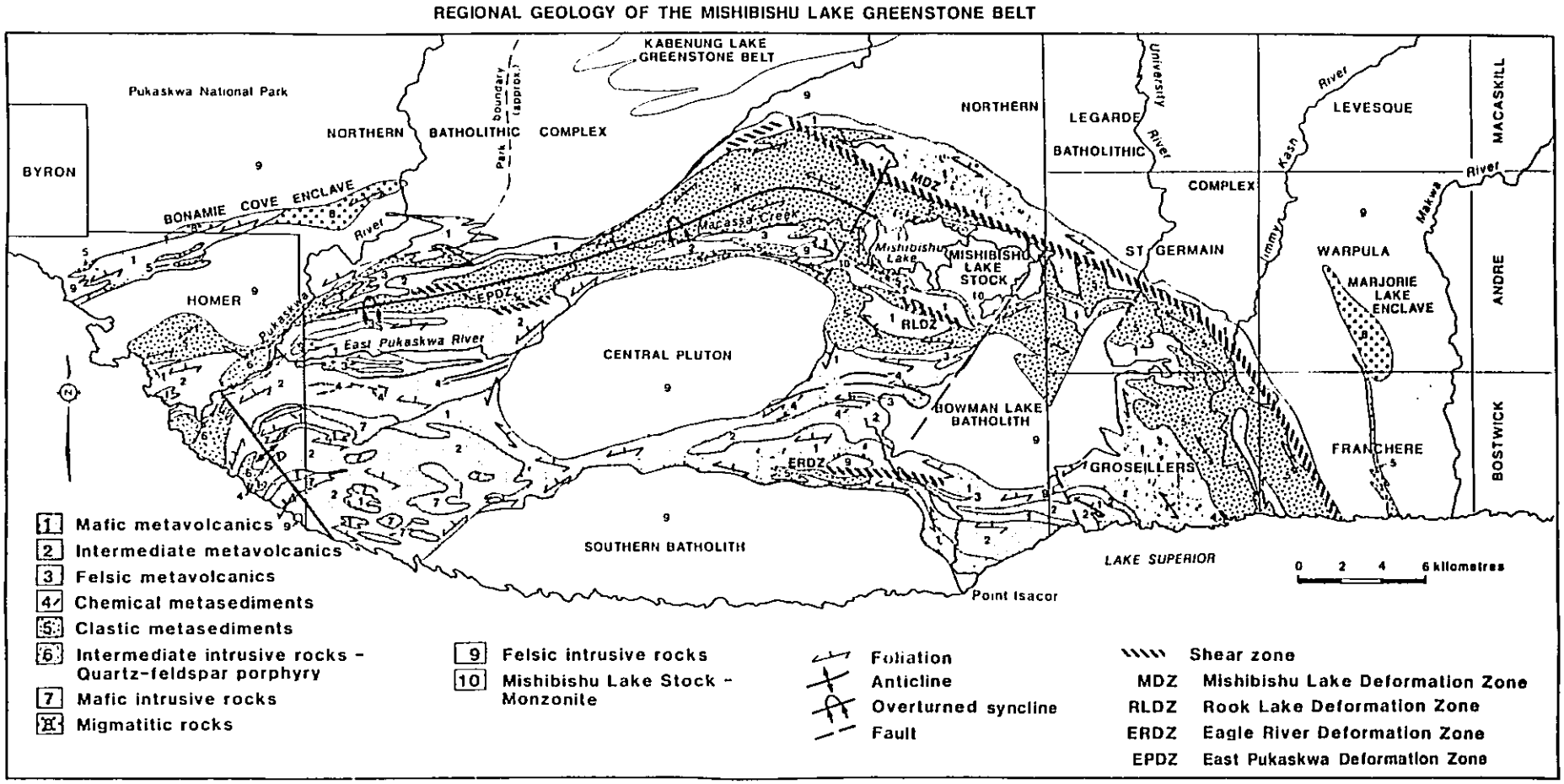

Figure 2. Geological sketch map illustrating the prominent structural features of the Mishibishu greenstone belt (Reid et al., 1989).

CHAPTER III

THEORETICAL ASPECTS OF U-Pb GEOCHRONOLOGY

The ages in geochronological studies are based on the decay of a radioactive parent atom to a stable daughter atom. According to Rutherford and Soddy (Faure (1986), the rate of this decay is proportional to the number of atoms, N, remaining at time t. Expressing this mathematically gives:

$$-\frac{dN}{dt} \propto N. \qquad (1)$$

Introducing the decay constant for a particular radionuclide into Equation (1) allows the decay rate of a radionuclide to be expressed as:

$$-\frac{dN}{dt} = \lambda N \ , \qquad (2)$$

Integrating Equation (2) gives:

$$-\int\frac{dN}{N} = \lambda\int dt \qquad (3)$$

$$-\ell n\ N = \lambda t + C, \qquad (4)$$

where C is a constant of integration. When $N = N_0$, for which $t = 0$, C may be solved for:

$$C = -\ell n\ N_0\ , \qquad (5)$$

Substituting into Equation (4) gives:

$$-\ell n\ N = \lambda t - \ell n\ N_0$$

$$\ell n\ \frac{N}{N_0} = -\ \lambda t, \qquad (6)$$

$$\frac{N}{N_0} = e^{-\lambda t}$$

$$N = N_0 e^{-\lambda t}. \qquad (7)$$

Equation (7) gives the number of radioactive parent atoms, N, remaining at any time t of an original amount of atoms, N_0, that were present at $t = 0$.

If the decay of a radioactive parent produces a stable radiogenic daughter, and at $t = 0$ there are no daughter atoms present, then the number of daughter atoms produced by decay of the parent at any time t is given by:

$$D^* = N_0 - N \qquad (8)$$

where D^* is the number of radiogenic daughter atoms produced.

In practice, it is convenient to relate the number of radiogenic daughter atoms to the number of parent atoms remaining, instead of the number of parent atoms to start. If N_0 is replaced by $Ne^{\lambda t}$ in Equation (8), the result is

$$D^* = Ne^{\lambda t} - N$$

$$D^* = N(e^{\lambda t} - 1) \qquad (9)$$

where D* is the number of radiogenic daughter atoms. In general, the total number of daughter atoms in a system is:

$$D = D_o + D^* \qquad (10)$$

where D is the total number of daughter atoms produced by decay of the parent, and D_o is the original number of daughters present at time t = 0.

Substituting Equation (10) into Equation (9) produces the basic age equation:

$$D = D_o + N(e^{\lambda t}-1) \qquad (11)$$

which may be solved algebraically for t:

$$t = \frac{1}{\lambda} \ \ell n \ (\frac{D-D_0}{N} + 1). \qquad (12)$$

The U-Pb Method of Dating

The U and Pb isostopes in this method are measured most frequently in the mineral zircon ($ZrSiO_4$). Elements U and Th substitute for Zr in the crystal structure, because of their similar ionic radii and charge. Inherited common Pb is almost entirely excluded from the crystal structure because of its larger ionic radius and lower charge than Zr. Therefore, zircon contains very little Pb at the time of its formation. Once formed, however, zircon shows excellent retention of U, Th, the intermediate daughters of these decay series, and radiogenic Pb. The high U and Th

content with respect to Pb within zircon makes this mineral a sensitive geochronometer. Measurable amount of U, up to several hundred parts per million, may be present in a single zircon crystal.

The decay of ^{238}U, ^{235}U, and ^{232}Th results in a series intermediate daughters which ultimately decay to ^{206}Pb, ^{207}Pb respectively. The decay for each radioactive parent can be summarized as:

$$^{238}U \rightarrow {}^{206}Pb + 8\ He + 6\beta^-$$

$$^{235}U \rightarrow {}^{207}Pb + 7\ He + 4\beta^-$$

$$^{232}Th \rightarrow {}^{208}Pb + 6\ He + 4\beta^-.$$

More detailed explanation of the above theory can be found in Faure (1986).

Since the half-lives of the parents are much larger than those of their respective intermediate daughters, the decay series achieve secular equilibrium. For a closed system in secular equilibrium, the production rate of the stable daughter at the end of the chain equals the rate of decay of its parent at the start of the chain.

There are four naturally occurring Pb isotopes:

$$^{208}Pb,\ ^{207}Pb,\ ^{206}Pb,\ \text{and}\ ^{204}Pb.$$

Only ^{204}Pb is not radiogenic and is used as a reference isotope. Thus, the isotopic composition of Pb in minerals containing U can be expressed as:

$$\frac{^{206}Pb}{^{204}Pb} = \left(\frac{^{206}Pb}{^{204}Pb}\right)_i + \frac{^{238}U}{^{235}Pb}(e^{\lambda_1 t}-1) \qquad (13)$$

$$\frac{^{207}Pb}{^{204}Pb} = \left(\frac{^{207}Pb}{^{204}Pb}\right)_i + \frac{^{235}U}{^{204}Pb}(e^{\lambda_2 t}-1) \qquad (14)$$

where i indicates the initial Pb isotope ratio of the mineral, and the remaining ratios represent those measured at the time of analysis. Both equations (13) and (14) may be solved algebraically for t after assuming reasonable values for initial Pb ratios:

$$t_{206} = \frac{1}{\lambda_1} \ell n \frac{\frac{^{206}Pb}{^{204}Pb} - \left(\frac{^{206}Pb}{^{204}Pb}\right)_i}{\frac{^{238}U}{^{204}Pb}} + 1 \qquad (15)$$

Equation (14) may be solved for t by similar methods. Both equations yield identical (i.e., concordant) ages if the following conditions are satisfied:

1. The mineral system remained closed to U, Pb and all intermediate daughters.
2. Initial Pb isotope ratios chosen are correct.
3. The decay constants of ^{238}U and ^{235}U are accurately known.
4. No change in the isotopic composition of U has occurred due to isotope fractionation or fission.
5. Analytical results are accurate and free of systematic errors.

Another age, which is useful in determining the age of a mineral which is not concordant, is based on the

$^{207}Pb/^{206}Pb$ ratio. This is derived by dividing Equation (14) by Equation (13) to give:

$$\left(\frac{^{207}Pb}{^{206}Pb}\right)^* = \frac{^{235}U}{^{238}U} \left(\frac{e^{\lambda_2 t}-1}{e^{\lambda_1 t}-1}\right) \qquad (16)$$

where $\left(\frac{^{207}Pb}{^{205}Pb}\right)^*$ is the radiogenic Pb ratio, corrected for initial Pb. This is a transcendental equation and cannot be solved for t by algebraic methods. A solution may be found by successive approximations of t until a value is found that solves the equation within the desired level of precision.

The U-Pb Concordia Diagram

The concordia diagram, developed by Wetherill (1956), represents both a graphical and mathematical solution for the discordant ages inherent in the U-Pb method. The decay of ^{238}U to ^{206}Pb and ^{235}U to ^{207}Pb described by equations (13) and (14) may be rewritten as:

$$\frac{^{206}Pb^*}{^{238}U} = e^{\lambda_1 t} - 1 \qquad (17)$$

$$\frac{^{207}Pb^*}{^{235}U} = e^{\lambda_2 t} - 1 \qquad (18)$$

where $^{206}Pb^*$ and $^{207}Pb^*$ are, as previously defined radiogenic daughter atoms. On the concordia diagram, the $^{206}Pb/^{238}U$ ratio is plotted on the ordinate and the $^{207}Pb/^{235}U$ ratio is plotted on the abscissa. Equations (17) and (18) are parametric equations on the curve that

is the locus of all concordant U-Pb systems. The curve, called the "concordia", is shown in Figure 3, and each point on the concordia represents a specific age for a concordant mineral.

For crystals representing systems that are not completely closed throughout their history, some Pb loss or U gain will cause the points representing the systems to plot below or above concordia. Loss of Pb causes the points to move along a chord towards the origin. This chord is called the "discordia" (Wetherill 1954), because all systems on such a chord have discordant ages. Wetherill showed that different zircon crystals from the same rock plotted as points on the discordia, and had a linear relationship due to the similar isotopic composition of Pb. Different zircons lose Pb at different rates, which causes them to be displaced along a line towards the origin along the discordia. Extrapolating the discordia provides two points of intersection with the concordia. The upper intercept represents the primary age of the mineral or rock, while the lower intercept relates to a younger event that caused the discordancy. Cases explaining the significance of the lower intercept are discussed in the following section on Pb loss.

Pb-loss Models

The amount of Pb lost appears to be related to the size of the zircon crystal, U content, and radiation damage of

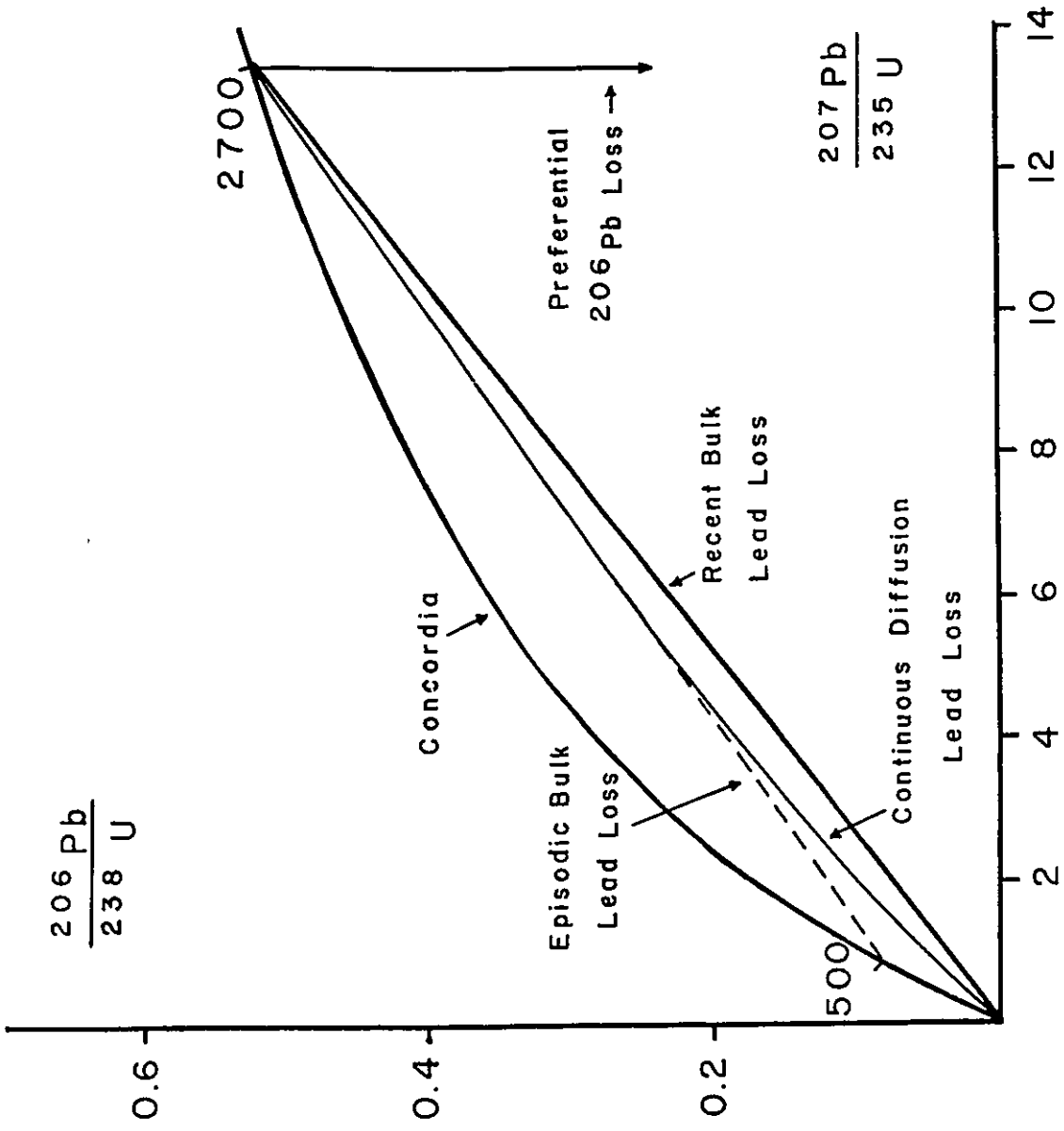

Figure 3. Concordia diagram showing the various models of Pb loss (Doe 1970).

the crystal. Smaller grains, and those with high U content, generally have larger Pb loss than larger grains, and those with lower U concentrations.

Although Pb is lost from zircons, it is still possible to extrapolate the discordia to determine an age for the formation of a mineral. There are essentially three models which explain Pb loss, all of which will produce the same primary age.

1. Episodic Pb Loss

This is the simplest model, in which a zircon loses Pb due to episodic events, such as metamorphism and chemical weathering. This Pb loss occurs in a much shorter time span with respect to the total time since crystallization (Wetherill 1956). On a concordia diagram, the discordia has an upper intercept giving the true age of the rock, and a lower intercept representing the time since episodic Pb loss. An example is given in Figure 3, for a rock which formed 2700 Ma ago and experienced an episode of Pb loss 500 Ma ago. At the time of crystallization (t = 0), the U/Pb ratios in the zircons plot at the origin, since there is no radiogenic Pb present. The U-Pb systems then evolved along the concordia curve until the Pb-loss event at 500 Ma. The zircons are displaced from the point on concordia that is the age of the rock (2700 Ma), towards the origin. If all the Pb was lost, the displacement would be right to the origin, leaving no evidence of the age of

original crystallization. Where only a fraction of the Pb was lost, the displacement of the points would be along a chord connecting the time of the Pb-loss event and the origin. When closure of the system is once again achieved, the U/Pb ratios continue evolving, but along parallel concordia curves, until the present. The discordia line fitted through the points is effectively rotated, with the upper intercept intersecting the primary age of the rock (2700 Ma), and the lower intercept indicating the time since the episode of Pb loss occurred (500 Ma) before present.

2. Continuous Diffusion

This model proposes that Pb loss was continuous through time, and not due to an episodic event. Tilton (1968) reported that U-bearing minerals from five continents have $^{207}P/^{206}Pb$ dates greater than 2300 Ma which plot on a single discordia line (Figure 4). This indicates an age of crystallization of 2800 Ma and episodic Pb loss around 600 Ma. The lower intercept implies that there was a worldwide metamorphic event 600 Ma ago, for which there is no geologic evidence. The episodic model suggests that a negligible amount of Pb was lost in these minerals between 2800 Ma to 600 Ma ago, despite evidence from other dating methods that indicates magmatic activity occurred during this time interval.

An alternative explanation for Pb loss was introduced by Tilton (1960) that is based on continuous diffusion of

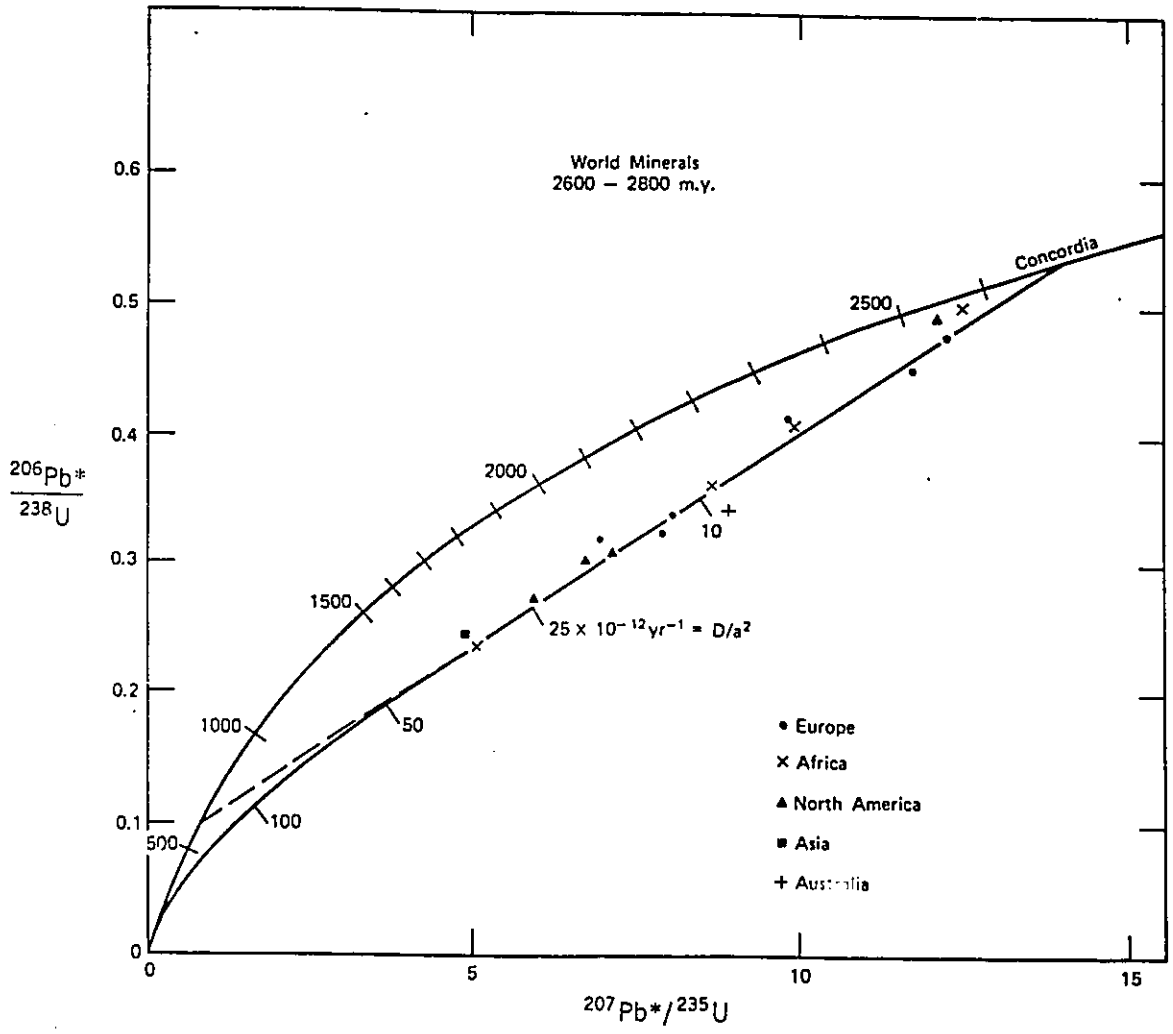

Figure 4. Concordia plot for minerals from different continents, illustrating the continuous diffusion model (Tilton 1960).

Pb from crystals at a rate controlled by a diffusion coefficient D, the effective radius 'a', and the concentration gradient. The assumptions in this model are that the crystals are spherical with an effective radius 'a', that U is uniformly distributed within the spheres, that the diffusion coefficient D is a constant through time, that diffusion of U and intermediate daughters is negligible with respect to Pb, and that diffusion follows Fick's Law. Tilton used these assumptions to derive an equation relating the daughter to parent ratio of a mineral to D/a^2 and t, where t is the age of the mineral. The solutions of the diffusion equation generate curves on the concordia diagram which are the loci of points representing the ages of U-Pb systems that have continuously lost Pb governed by the parameter D/a^2. The discordia line will be linear until it approaches the origin, where it becomes non-linear. Extrapolation of the discordia to get an upper intercept still represents the age of the crystal, but the lower intercept has no geological significance in this model, since it is only a linear extrapolation of the chord trajectory. It should be noted that preferential loss of one type of Pb over another, such as loss of ^{208}Pb over ^{206}Pb and ^{207}Pb, results in points plotting along a discordia that also does not pass through the origin. The lower intercept, in this situation, also has no geological significance.

3. Dilatancy Model

This model proposes that U-bearing minerals suffer radiation damage due to alpha-decay of U, Th, and their daughters (Goldich and Mudrey 1972). The amount of radiation damage to the minerals increases with age, and with its U and Th content. The damage causes microcapillary channels to form that allow water to enter the crystal. The water is tightly held until confining pressure on the minerals is released by uplift. The resulting dilatance of the zircons allows the water and dissolved Pb to escape. The lower intercept on the concordia for this model indicates the time of uplift and erosion of rocks in a given region. The dilatancy model also provides a feasible explanation for the lower intercept of 600 Ma described by Tilton (1960), without the occurrence of continuous diffusion.

Loss of Intermediate Daughter Elements

The decay of U to Pb produces a variety of intermediate daughter products, including Rn gas, which may leak from the zircon crystal structure. Normally, with simple Pb loss, the discordant ages for the U-Pb system in zircons increase in the order of $^{206}Pb/^{238}U$, $^{207}Pb/^{235}U$, and $^{207}Pb/^{206}Pb$ where the $^{207}Pb/^{206}Pb$ age is the minimum age of the rock. The loss of Rn is evident as a pattern of discordant ages, where the $^{207}Pb/^{206}Pb$ age is greater than the true age of the rock,

and the $^{206}Pb/^{238}U$ age is less than the true age. In this case, the true age of the rock is given by $^{207}Pb/^{235}U$ age. In the ^{238}U-^{206}Pb series ^{222}Rn, with a half-life of 3.8 days, is more likely to be lost than ^{219}Rn in the ^{235}U-^{207}Pb series, which has a half-life of only 3.9 seconds (Wetherill 1953). This may also indicate that fractionation of isotopes has occurred, causing a preferential loss in one Pb isotope over another. This model leaves the upper intercept unchanged, but displaces the lower intercept towards the origin, and it also accounts for the negative intercepts encountered in some zircon age studies.

CHAPTER IV

ANALYTICAL TECHNIQUES

Twenty-five samples in total were collected, but only seven of these contained sufficient zircons for analysis. Each sample consisted of approximately 50 kg of fresh, unaltered rock where possible. Some weathered surfaces were unavoidable, but this material does not affect the analytical precision of the samples. The samples were crushed and pulverized to -60 mesh size and heavy minerals were separated using a Wilfley table. Coarse magnetic separation of zircons was achieved using a Carpco magnetic separator, and these were further concentrated by sinking in heavy liquids and subsequent boiling in 50% nitric acid. The zircon concentrate at this stage was separated into various magnetic fractions by magnetic susceptibility using a Frantz isodynamic magnetic separator, and then sieved into size ranges from +70 to -325 mesh. The best crystals were handpicked from all zircon subsamples, and when necessary, air abraded (Krogh 1982) for at least one hour to produce more concordant data points. Abrading removes encrusted mineral fragments or metamorphic growth rims from the zircon crystals.

Zircons were dissolved in teflon pressure vessels at a

temperature of 195°C for one week, with ultrapure HF and HNO_3 acids using a modified method after Krogh (1973). All reagents were purified by the subboiling distillation technique described by Mattison (1972). Aliquots of the dissolved samples were taken and spiked with a mixed ^{208}Pb - ^{235}U tracer, then taken to dryness and stored in 5mL teflon beakers. Separation of U and Pb was achieved on an ion exchange column. Techniques for U-Pb chemistry are provided in Appendix B. Samples were loaded onto a rhenium filament using a silica gel and phosphoric acid, and isotopic ratios were measured on a six-collector, extended-focus, 54 cm VG Sector mass spectrometer at the Isotope Geochemistry Laboratory, University of Kansas. The $^{208}Pb/^{206}Pb$, $^{207}Pb/^{206}Pb$, and $^{235}U/^{238}U$ ratios are suitably measured on the Faraday collectors in the static mode. Due to the low intensity of the ^{204}Pb signal, this peak is measured on a Daly collector, while the ^{206}Pb peak is simultaneously measured on a Faraday collector. The Daly collector is cross-calibrated to the Faraday cup, and thus, a $^{204}Pb/^{206}Pb$ ratio may be determined. This calibration procedure is performed for each unspiked aliquot prior to taking blocks of data. Cross-calibration between the four Faraday collectors used is normally required only once each day before any data is taken. Much greater accuracy and precision is possible using the multiple collector scheme, since peak switching is eliminataed, and therefore, any

change in ion beam current will be seen simultaneously by all collectors. A mass fractionation of 0.12% bias per mass unit was applied to the Pb data. Radiogenic ^{207}Pb and ^{206}Pb are calculated by correcting for modern blank Pb, and for nonradiogenic initial Pb using the model Pb composition of Stacey and Kramers (1975). Analytical ^{206}Pb blanks were 1ng or less, and 0.25 ng or less for U. The decay constants used to calculate the ages of the rocks were 0.155125×10^{-9} year^{-1} for ^{238}U (λ_1), and 0.98485×10^{-9} year^{-1} (λ_2) for ^{235}U (Steiger and Jäger 1977). The U/Pb ratios are accurate to ±1.0% at 2-sigma. Concordia intercepts were calculated based on the regression and error analysis method of Ludwig (1982b). The $^{207}Pb/^{235}U$ and $^{206}Pb/^{238}U$ ratios have 2-sigma uncertainties of ±1.0%, with a correlation coefficient of 0.98.

The regression of Ludwig (1982b) is based on that of York (1969). If the probability of fit of the data points is 30% or greater, then a Model 1 solution is automatically provided, giving greater weighting to the more concordant points. Where data points fall outside analytical error (probability of fit less than 30%) a Model 2 solution is selected, which gives all points equal weighting, and yields higher uncertainties. All ages are given with 2-sigma error limits.

CHAPTER V

STATISTICAL ANALYSIS AND TREATMENT OF ERRORS

Many of the current age dating methods require fitting a straight line through a set of data points. Historically, the first method of fitting a straight line was visual. Improvements in accuracy and precision resulted by using the simple "least-squares" regression (Acton 1959), which was applied to Rb-Sr isochrons in the early 1960's. The problem in using such a regression is that deviations from the best straight line are assumed to result from error in one coordinate axis only (X or Y), and that the other coordinate axis is free from errors. This problem was overcome when McIntyre et al. (1966) derived a least-square cubic equation, which employs a system of weighted points for fitting isochrons in the Rb-Sr age dating method. York (1966) derived a similar equation independently, which is used in Pb-Pb age work. Brooks et al. (1972) modified the error treatment on the McIntyre et al. (1966) regression. For U-Pb ages, Ludwig (1980, 1982b) utilized the York (1969) regression to find concordia intercepts, and derived equations for the estimation and correlation of errors associated with U-Pb isotope data, based on work by Cummings (1969, 1972). Subsequently, Davis

(1982) formulated a regression based on York (1969), but employed an error propagation function used by physicists. Because this error function was not specifically designed to take into account all uncertainties involved in the U-Pb method, the Davis (1982) regression, as published, does not always work, and does not generate lower intercept errors. Currently, the regressions and related error treatments most accepted, are those by McIntyre et al. (1966) for Rb-Sr and Nd-Sm, York (1969) for Rb-Sr in North America, and Pb-Pb , and Ludwig (1982b) for the U-Pb concordia.

Errors and Error Treatment

The type of uncertainties encountered in U-Pb isotope data are of analytical and geologic nature. Analytical errors include those in the chemistry used to extract U and Pb from the zircons, uncertainties in initial-Pb and blank-Pb amounts and isotopic composition, and mass-discrimination in mass spectrometer runs. Most analytical errors tend to cancel out, and geological uncertainties, once determined, are usually constants for a given area (Ludwig 1980).

As stated previously, the simple regression is inadequate for use on U-Pb data points, because error is assumed in one axis (X or Y) only. In analytical work, there is a covariance between X and Y, which are not totally independent, and thus uncertainties exist in both the X and Y axis. The point which is farthest from the

origin has the largest error, and thus introduces large uncertainties in determining the best fit of the line in the simple regression, which is opposite of what is desired for concordia plots. The point closest to concordia should have the smallest error, thus confining the upper intercept age within narrow limits of uncertainty. The Least-square Cubic regression allows appropriate weights to be assigned to data in the $^{207}Pb/^{235}U$ (X) and $^{206}Pb/^{238}U$ (Y) coordinates. In U-Pb work, this best-fit line is the discordia. The critical measurements for determining the age are the $^{204}Pb/^{206}Pb$ and $^{207}Pb/^{206}Pb$ ratios, which are measured directly. The uncertainties in the data are depicted as error-envelopes shaped like irregular hexagons or ellipses on a concordia diagram. The errors are propagated along a line passing through the origin and the major axis of the error-envelope. This line, if extrapolated to intersect the concordia curve, will yield the $^{207}Pb/^{206}Pb$ age of the zircon point.

Uncertainties in the concordia-intercept ages are determined by first calculating a mean or "centroid" for the weighted points along the discordia (best-fit line). An error-envelope is associated with the best-fit line, which takes the form of a hyperbola, symmetrical along the Y-axis about the line. The least separation is at the centroid of the best-fit line, where the error of fit is a minimum. The intercepts with concordia of the error-envelope are the

uncertainties in the age at the 2-sigma level (Ludwig 1980, 1982b).

CHAPTER VI

RESULTS

The location of the analyzed samples are shown in Figure 1 and Appendix D, and petrographic descriptions and zircon photos are in Appendix C. The ages with associated 2-sigma errors are calculated using the regression and error treatment of Ludwig (1982b). All results are shown in Tables 2 and 3, and Figures 5 to 11.

Jostle Lake tonalite (G15)

A tonalite from the Northern Batholithic complex was collected near Jostle Lake, about 12 km east of Mishibishu Lake. This yielded a Model 1 age of 2721.2 ± 4.1 Ma (Figure 5) with a probability of fit of 36 percent for four zircon fractions (Tables 2 and 3), which are all clear to brown in colour, and crystal morphology range from euhedral to rounded. The fraction with rounded zircons was virtually concordant.

Chimney Point porphyry (G25)

A subvolcanic porphyry near Chimney Point at the western boundary of the Mishibishu greenstone belt contains clear to pink translucent zircons which are cracked, and some show evidence of containing xenocrystic cores

Table 2. Analytical Data for Zircons from the Mishibishu Greenstone Belt

Sample Detail					Concentration (ppm)		Atomic Ratios				
Sample Number		Magnetism and type	Tyler Mesh Grain Size	Sa.Wt. (mg)	U	Pb	$^{204}Pb/^{206}Pb$ [a]	$^{208}Pb/^{206}Pb$ [b]	$^{207}Pb/^{206}Pb$ [b]	$^{207}Pb/^{235}U$ [c]	$^{206}Pb/^{238}U$ [c]
G15	A	NM0° Hp, El	-100 + 200	0.5	349	206	0.001495	0.11927	0.20335	13.1466	0.5092
	B	NM0° Hp,Rd	-100 + 200	0.5	147	88	0.001605	0.11050	0.20209	13.4802	0.5220
	C	NM0° Hp,Fr	-100 + 200	0.9	168	91	0.000454	0.07228	0.18956	12.8074	0.4980
	C1	M1° Hp	-100 + 200	1.1	175	94	0.000309	0.08265	0.18788	12.5710	0.4899
G25	A	NM0° Hp	-100 + 200	0.6	219	121	0.000306	0.16468	0.18268	11.9477	0.4762
	B	M0° Hp	-100 + 200	0.2	559	308	0.000165	0.16527	0.18110	11.8734	0.4755
	C	M1° Hp	-100 + 200	0.4	227	118	0.000401	0.16082	0.17923	11.1349	0.4513
	A1	NM0° Ab, Hp	-100 + 200	0.6	172	106	0.002863	0.25021	0.21235	11.8100	0.4734
	B1	M1° Ab, Hp	-100 + 200	0.7	91	48	0.000719	0.17066	0.18131	11.0397	0.4471
G22	A1	NM0° Ab,Hp	-100 + 200	1.0	49	28	0.000690	0.11727	0.81371	12.6206	0.5005
	B1	M0° Ab,Hp	-100 + 200	0.6	85	46	0.000651	0.11314	0.18187	12.1523	0.4855
	C1	M1° Ab,Hp	-100 + 200	0.8	120	60	0.001102	0.13135	0.18557	10.6357	0.4371
G4	A	M0° Hp	-100 + 200	0.3	113	64	0.000663	0.11570	0.18253	12.7354	0.5060
	B	M1° Hp	-100 + 200	0.5	99	56	0.000806	0.12047	0.18453	12.5545	0.4996
	C	M3° Hp	-100 + 200	0.5	129	72	0.000328	0.11276	0.18251	12.5609	0.4992
	D	M5° Hp	-100 + 200	0.5	96	54	0.000805	0.12619	0.18437	12.4507	0.4950
G14	A	M1° Ab, Hp	-100 + 200	1.1	886	443	0.001707	0.13803	0.19648	10.3071	0.4249
	B	M0° Hp	-200 + 325	1.0	397	193	0.001158	0.13340	0.18869	10.1665	0.4200
	C	M0° Hp, Am	-100 + 200	0.5	282	154	0.001650	0.14527	0.19622	11.4088	0.4628
	D	M0° Hp, Cl	-100 + 200	0.5	1031	500	0.001126	0.11426	0.19066	10.2556	0.4243
	E	NM0° Hp	-100 + 200	0.6	1542	747	0.001005	0.11130	0.18802	10.3777	0.4273

Table 2 (cont'd)

Sample Detail					Concentration (ppm)		Atomic Ratios				
Sample Number		Magnetism and type	Tyler Mesh Grain Size	Sa.Wt. (mg)	U	Pb	$^{204}Pb/^{206}Pb$ [a]	$^{208}Pb/^{206}Pb$ [b]	$^{207}Pb/^{206}Pb$ [b]	$^{207}Pb/^{235}U$ [c]	$^{206}Pb/^{238}U$ [c]
G17	A	M0*	-100 + 200	0.6	1444	688	0.000432	0.12156	0.17798	10.1217	0.4239
	B	M1*	-200 + 325	0.3	968	452	0.000581	0.14170	0.17760	9.6955	0.4088
	C	M3*	-100 + 200	0.5	1594	720	0.000524	0.12375	0.17776	9.4647	0.4008
G16	A	NM0* Hp	-100 + 200	0.9	353	254	0.000177	0.45526	0.18298	12.7774	0.5092
	B	M0* Hp	-100 + 200	1.1	238	164	0.000138	0.48065	0.18214	12.0767	0.4813
	C	M1* Hp	-100 + 200	0.7	542	390	0.000095	0.50442	0.18207	12.4329	0.4956
	D	M3* Hp	-100 + 200	0.7	526	363	0.000088	0.46681	0.18187	12.1731	0.4855

Notes: For magnetic susceptibility, M = magnetic, NM = nonmagnetic at given angle of the Frantz isodynamic separator at 1.7A field current. H = handpicked, Ab = abraded, El = elongate, Rd = rounded, Fr = fractured, Cl = cloudy, am = amber

[a] Raw ratio; [b] Blank corrected; [c] Blank and nonradiogenic Pb-corrected

Table 3. U-Pb Age Data for Zircons from the Mishibishu Lake Greenstone Belt

Sample Number		Model Ages (Ma) $^{206}Pb/^{238}U$	Model Ages (Ma) $^{207}Pb/^{235}U$	Model Ages (Ma) $^{207}Pb/^{206}Pb$	Concordia Ages (Ma) Upper Intercept	Concordia Ages (Ma) Lower Intercept	Remarks
Jostle Lake tonalite							
G15	A	2653	2690	2718			
	B	2708	2714	2719	2721.2±4.1	420±170	Ludwig 1982b
	C	2605	2666	2712			Model 1
	C1	2570	2648	2708			p=36%
Chimney Point porphyry							
G25	A	2511	2600	2671			Ludwig 1982b
	B	2508	2595	2663			Model 2
	C	2401	2535	2643	2696.0±17.0	740±210	P=8%
	A1	2499	2590	2661			
	B1	2382	2527	2645			
Pilot Harbour granite							
G22	A1	2616	2652	2679			Ludwig 1982b
	B1	2551	2616	2667	2693.2±6.9	835±87	Model 1
	C1	2338	2492	2620			P=99%
David Lakes pyroclastic							
G4	A	2640	2660	2676			Ludwig 1982b
	B	2612	2647	2674	2676.7±6.9	140±530	Model 1
	C	2610	2647	2676			P=61%
	D	2592	2639	2675			

Table 3 - continued

Sample Number		Model Ages (Ma) $^{206}Pb/^{238}U$	Model Ages (Ma) $^{207}Pb/^{235}U$	Model Ages (Ma) $^{207}Pb/^{206}Pb$	Concordia Ages (Ma) Upper Intercept	Concordia Ages (Ma) Lower Intercept	Remarks
Tee Lake tonalite							
G14	A	2283	2463	2615			
	B	2260	2450	2611			
	C	2452	2557	2642	2673.0±12.0	634±96	Ludwig 1982b
	D	2280	2458	2609			Model 1
	E	2294	2469	2617			P=31%
Bowman Lake batholith							
G17	A	2278	2446	2589	2639±25	581±180	Ludwig 1982b
	B	2209	2406	2577			Model 1
	C	2173	2384	2570	2672	792	P=83%
							P=12% forced through 2673 Ma
Iron Lake gabbro							
G16	A	2653	2663	2671			Ludwig 1982b
	B	2533	2610	2671	2671.0±3.6	30±200	Model 1
	C	2595	2638	2671			P=87%
	D	2551	2618	2670			

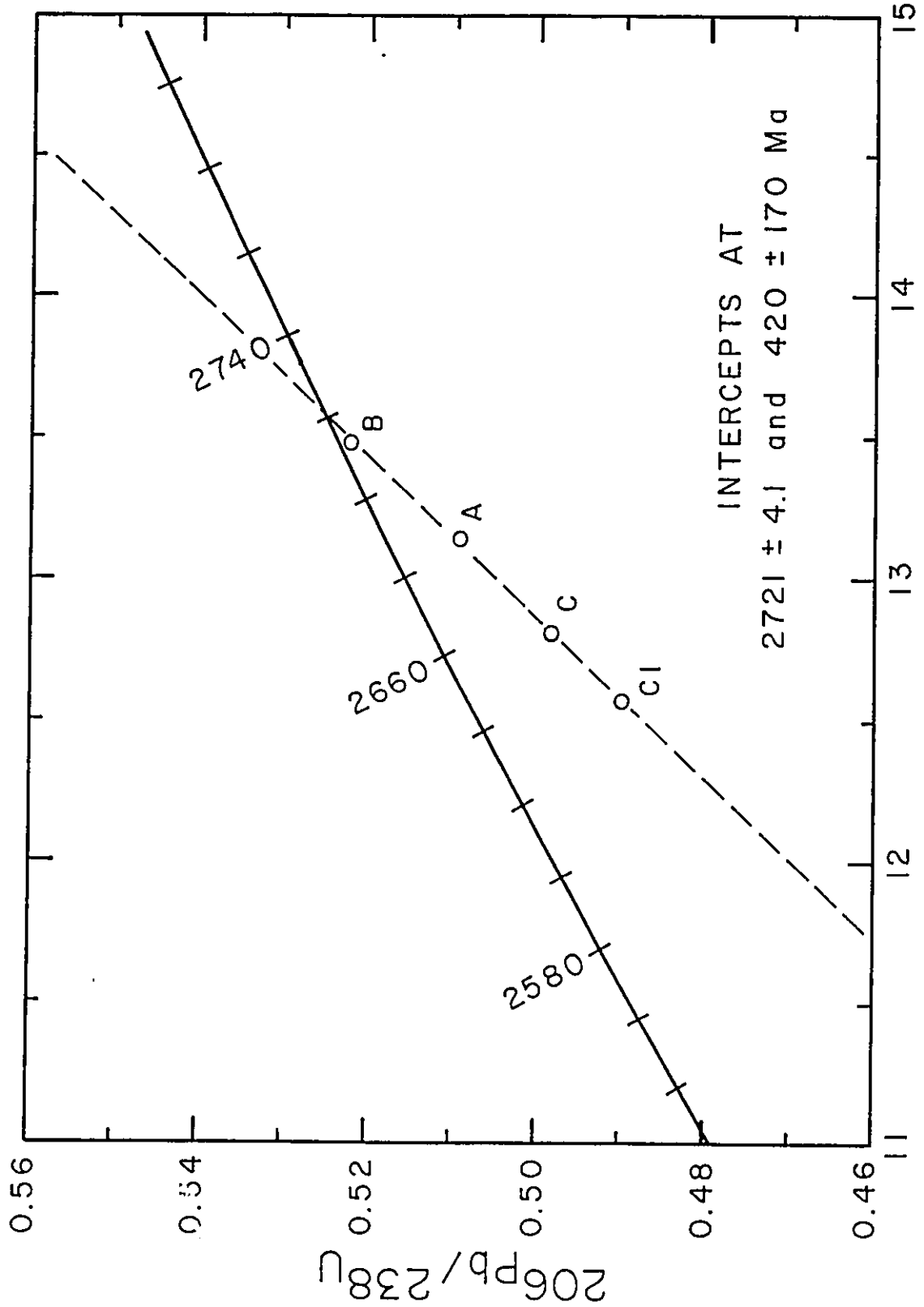

Figure 5. Concordia plot for the Jostle Lake tonalite (G15).

(Appendix C). Of the five fractions used to obtain an age, two were abraded. An upper intercept of 2696.0 ± 17 Ma was determined, which is a Model 2 age (Figure 6). The probability of fit was only 8 percent (Tables 2 and 3) and the points are about 10 to 15 percent discordant.

Pilot Harbour granite (G22)

At the southern boundary of the Mishibishu Lake belt is the Southern Batholith. A granite sample was taken at Pilot Harbour along the Lake Superior shoreline. Zircons from this pluton are subhedral, clear to translucent and generally crack-free. The Model 1 upper intercept age for three abraded fractions was 2693.2 ± 6.9 Ma (Figure 7), with 99 percent probability of fit (Tables 2 and 3). The discordancy of the points is between about 5 to 25 percent.

David Lakes pyroclastic (G4)

The foliated David Lakes pyroclastic was sampled about 5 km north of David Lakes. Zircons are euhedral, pastel brown in colour, and generally transparent. The four fractions used are within two percent of concordia, with two points virtually coinciding. These unabraded fractions give a Model 1 upper intercept age of 2676.7 ± 6.9 Ma (Figure 8) with a probability of fit of 61 percent (Tables 2 and 3).

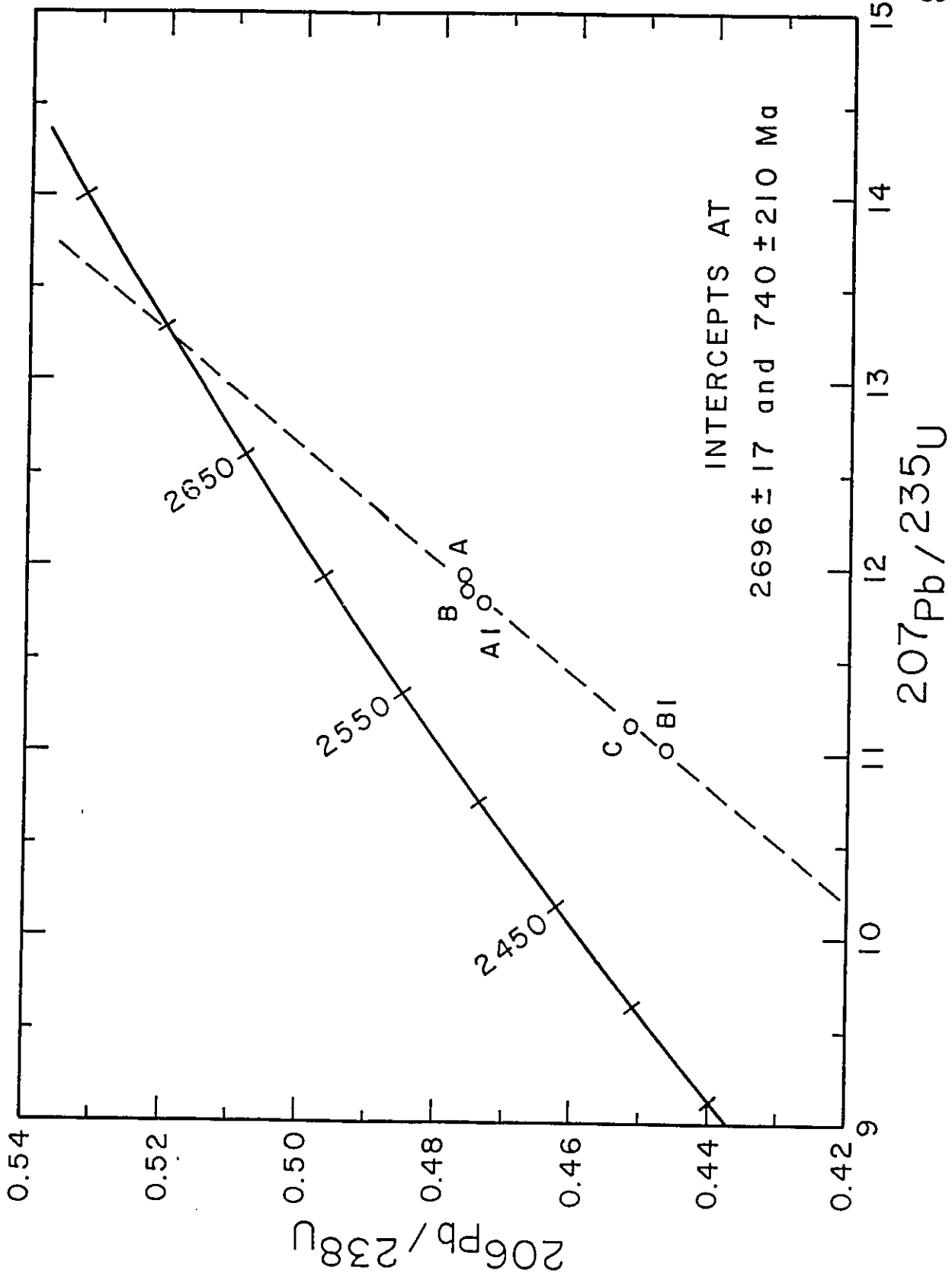

Figure 6. Concordia plot for the Chimney Point porphyry (G25).

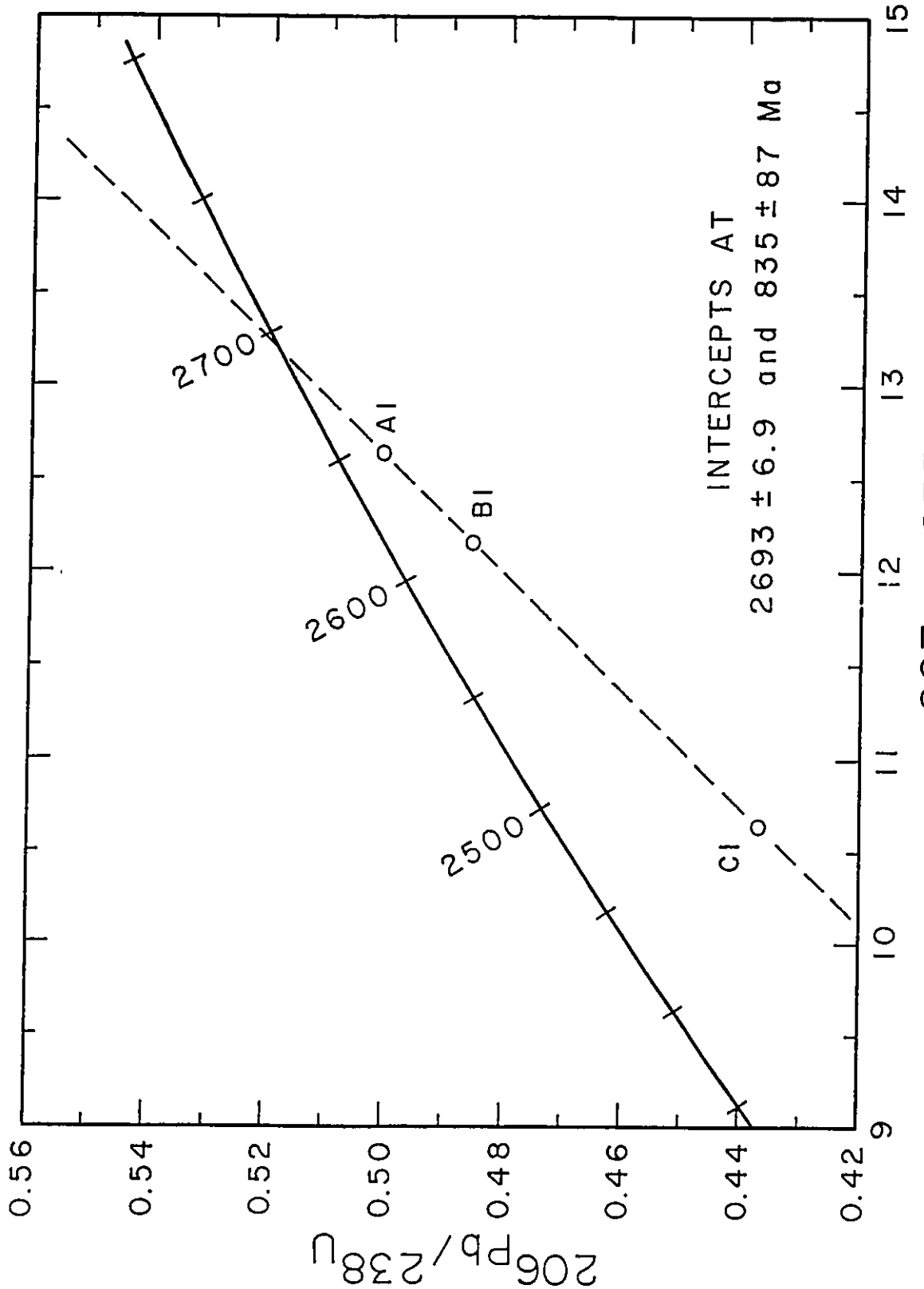

Figure 7. Concordia plot for the Pilot Harbour granite (G22).

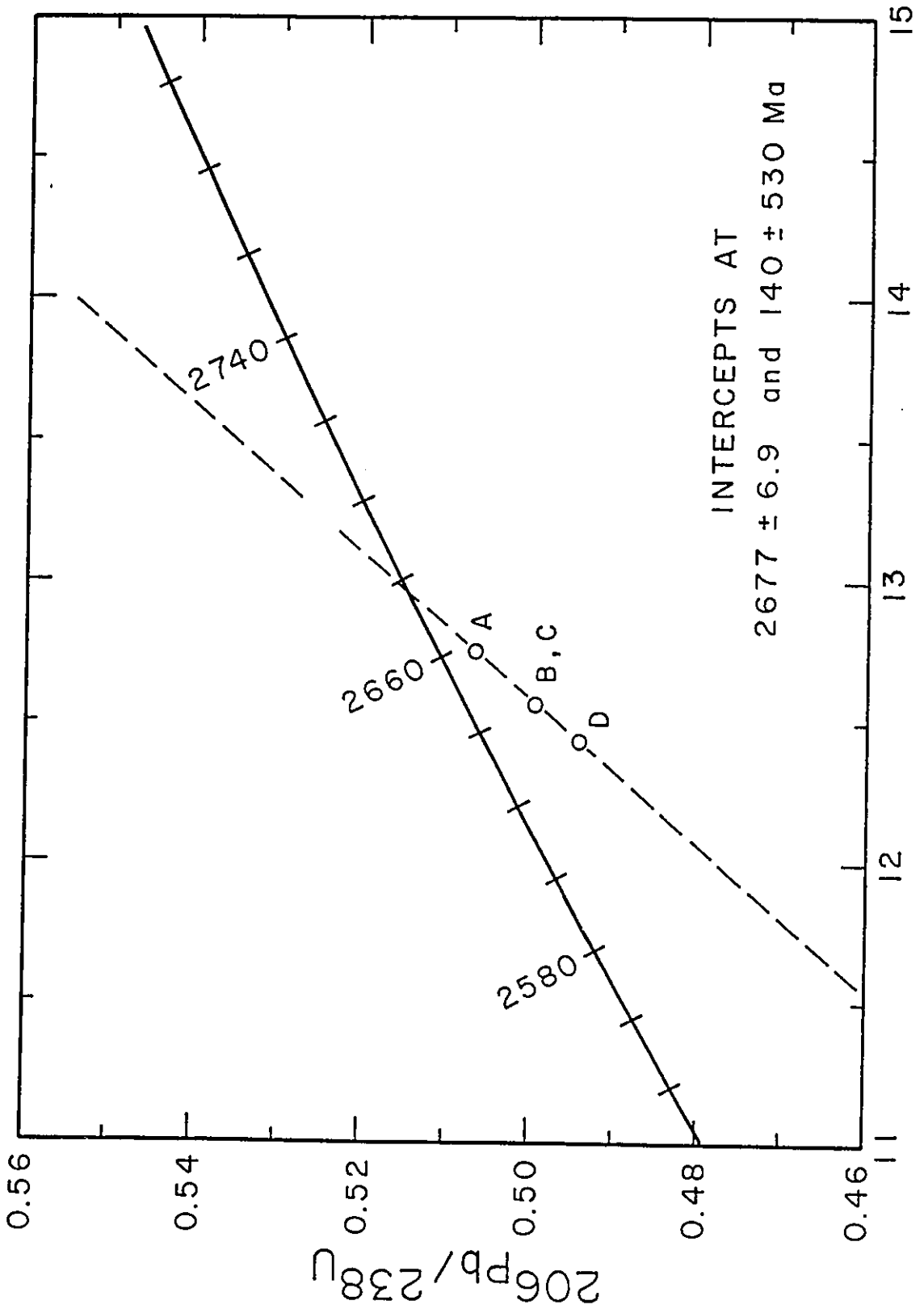

Figure 8. Concordia plot for the David Lakes felsic pyroclastic breccia (G4)

Tee Lake tonalite (G14)

A second tonalite from the Northern Batholithic complex was collected from the Tee Lake area, about 20 km west of Mishibishu Lake, and contains a variety of zircons ranging in colour from clear to amber, and milky white. The points are about 20 percent discordant, except for one fraction which is only about 10 percent discordant. The Model 1 upper intercept age is 2673.0 ± 12 Ma (Figure 9) with a probability of fit of 31 percent (Tables 2 and 3).

Bowman Lake granite (G17)

The Bowman Lake batholith was the only internal granitoid containing zircons of suitable quality and quantity for dating. This granite is located about 5 km south of Mishibishu Lake. Three fractions were obtained, the zircon crystals being translucent, pale brown to milky white in colour, and generally cracked. The upper concordia intercept was 2639.0 ± 25 Ma with 85 percent probility of fit (Figure 10 trajectory (a), Tables 2 and 3), which is a Model 1 solution. For geological reasons, this regression was forced through an age of 2673 Ma giving a probability of fit of 12 percent for a Model 2 upper intercept of 2672 Ma (Figure 10, trajectory (b), Tables 2 and 3). The points are 20 to 25 percent discordant, indicating significant Pb loss may have occurred, and thus introducing large uncertainty in the age.

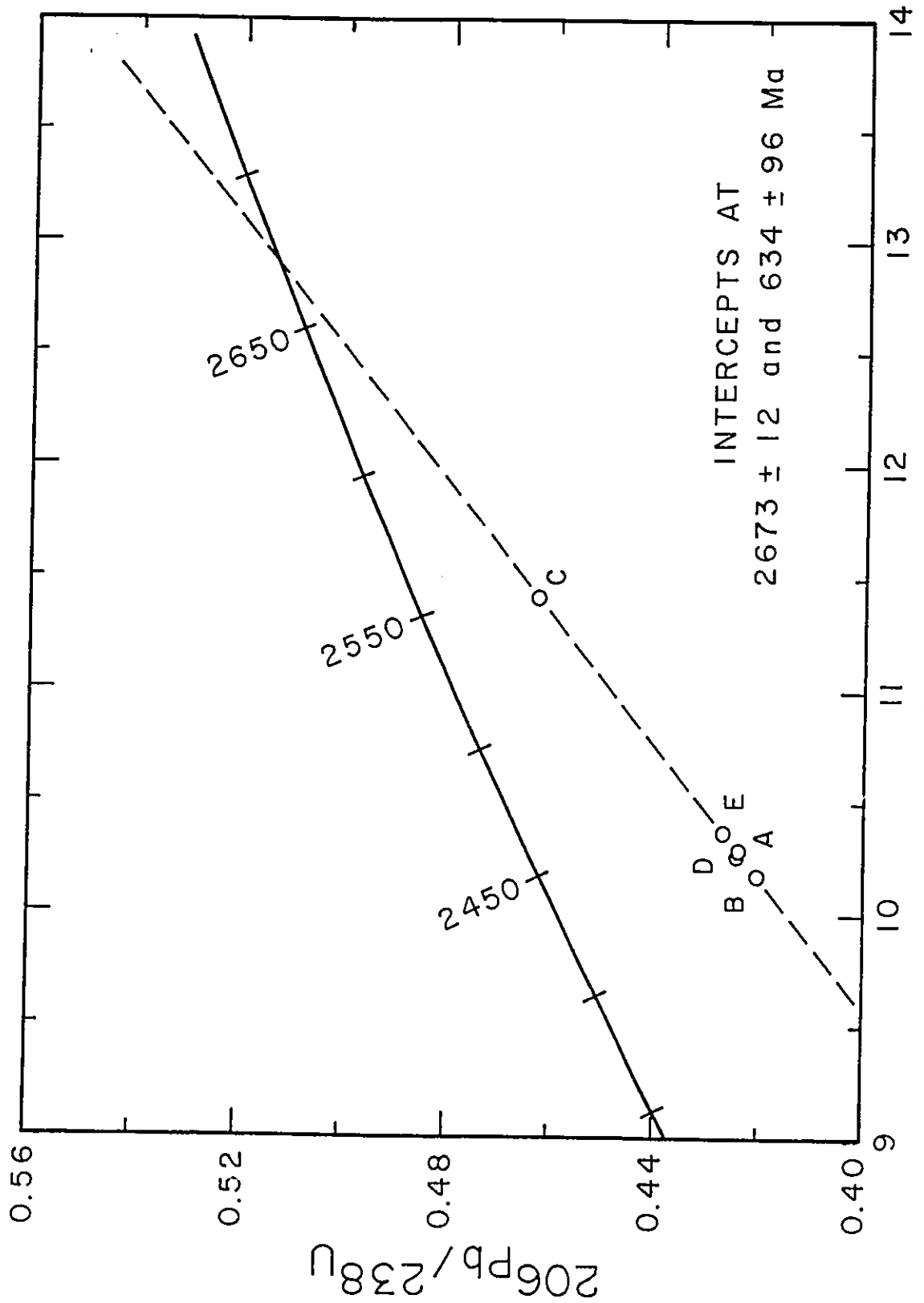

Figure 9. Concordia plot for the Tee Lake tonalite (G14).

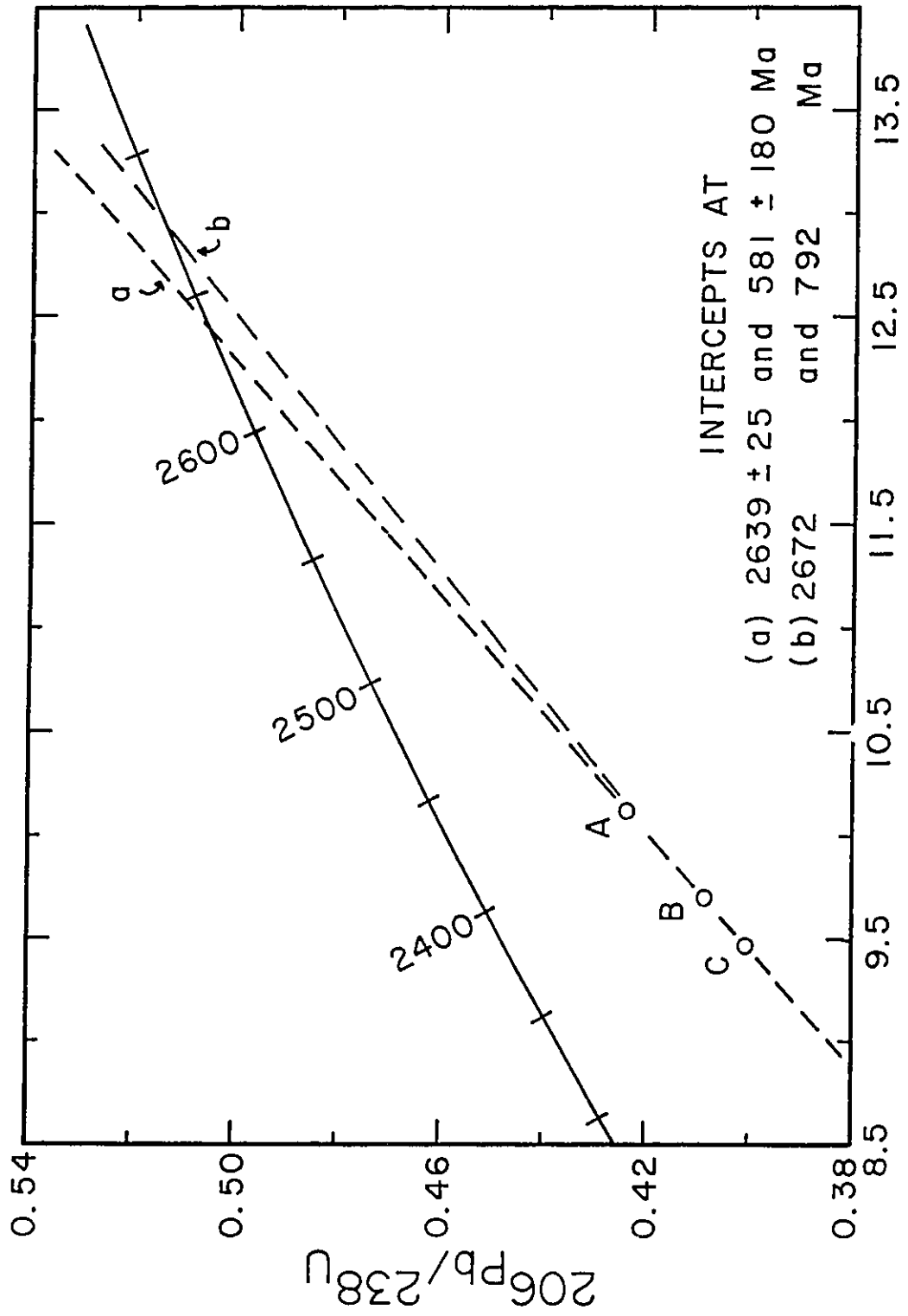

Figure 10. Concordia plot for the Bowman Lake granite (G17).

Iron Lake gabbro (G16)

The Iron Lake gabbro intrudes the southwest end of the Kabenung Lake belt and the Northern Batholith, and yielded fractured zircons which are pink to pastel brown in colour. The four fractions analyzed, one of which is concordant, gave a concordia age of 2671.0 ± 3.6 Ma (Figure 11) and a probability of fit of 87 percent (Tables 2 and 3).

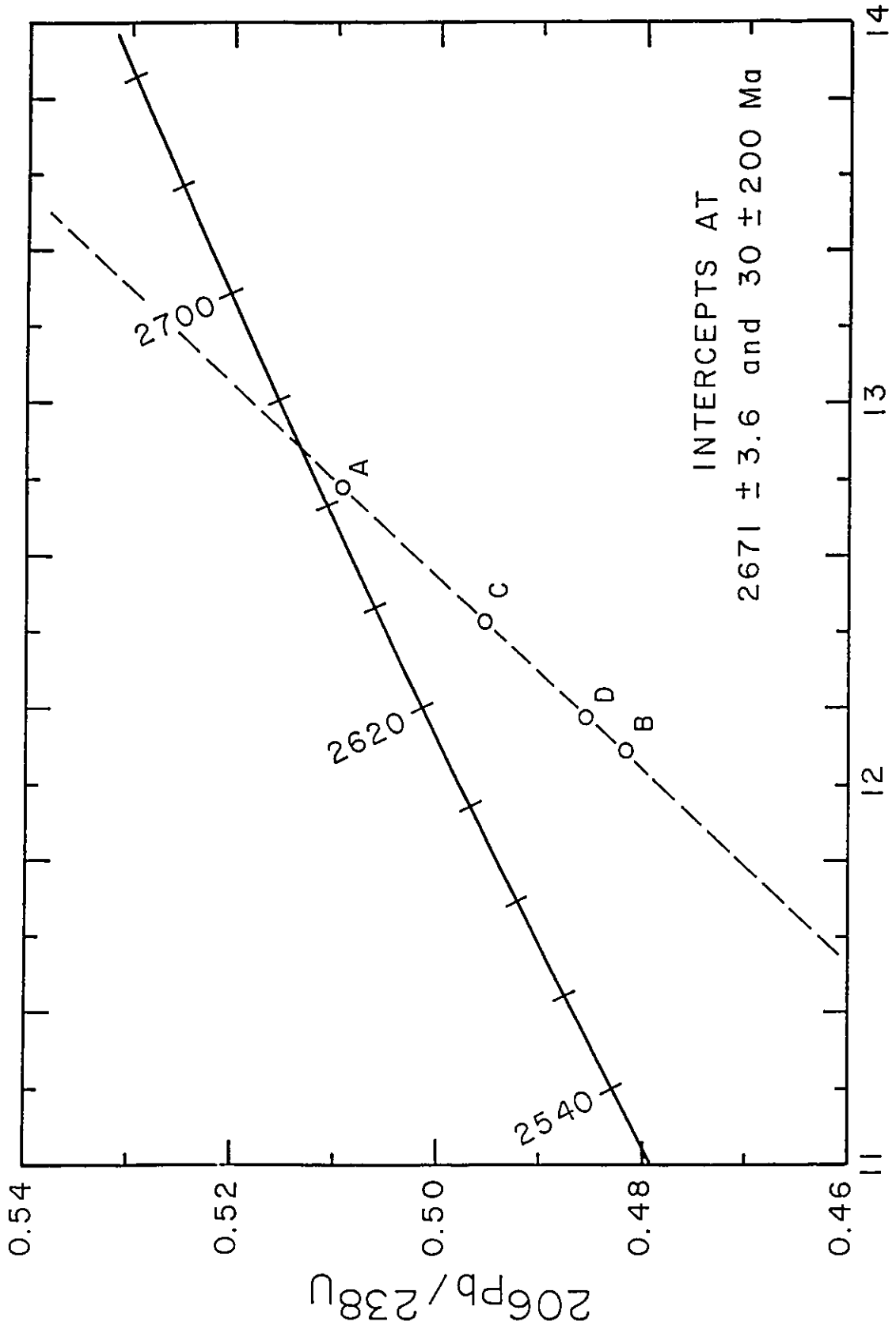

Figure 11. Concordia plot for the Iron Lake gabbro (G16).

CHAPTER VII

DISCUSSION

Five of the seven ages determined in this study are within experimental error and are clearly very precise ages, not only from an analytical point of view, but also from a geological perspective. The ages of the other two, the Chimney Point porphyry and the Bowman Lake granite, although outside analytical limits at the 95% confidence level, are still probably correct but at a lower level of confidence, which is apparent from their higher error uncertainties.

The Chimney Point porphyry zircons are of very good quality. Initially, three handpicked zircon fractions (A, B, and C, Table 2, Figure 6), were analyzed and were found to scatter. To improve the age, two additional fractions, A1 and B1 from fractions A and B, were abraded and handpicked. These two additional points failed to reduce the age uncertainty. In fact, they plot below points A and B which is contrary to expectation, as abrasion normally makes points more concordant and not less concordant as observed. This means that U and Pb are not uniformly distributed throughout the crystal, and that abrasion has selectively removed Pb. Also, the U and Pb content of

the abraded zircons is significantly lower than in the unabraded crystals, as shown in Table 2. This behavior indicates the possible presence of an older xenocrystic component or younger overgrowths. Subsequent examination of the zircons from this rock under the microscope revealed the possible presence of cores as shown in the photographs in Appendix C. Despite the observed scatter of the data, the 2696 ± 17 Ma age for this rock is considered correct, as it fits well with the ages for the upper volcanics as reported for the Wawa area (Turek et al. 1982, 1984, 1988).

The Bowman Lake granite is dated at ca. 2672 Ma which is an interpreted age (Figure 10, trajectory (b)). The younger age of 2639 Ma (Figure 10, trajectory (a)) may indicate that this is a post-tectonic pluton, although field relations do not provide proof of such a hypothesis. The three zircon fractions analyzed are collinear, but very discordant, and close together. Thus these points cannot yield a good age. The zircons from this rock, which is a high K granite, have high U content (Table 2) and therefore are of poor quality. The quantity of zircons which this rock produced was also poor, which precluded the analyses of additional fractions.

The ages determined in this study make sense chronostratigraphically, and do not contradict the geologic mapping of Reid and Reilly (1987) and Reid et al. (1989).

In fact, they provide additional evidence that the mapping is correct. A revised table of lithologic units (Table 4) of the Mishibishu area is subdivided into categories of supracrustal and plutonic rocks based on the ages from this study. This table in no way violates geologic field relations seen in the area. Furthermore, the ages reported here are comparable to the ages reported for the Michipicoten and Gamitagama greenstone belts (Turek et al. 1982, 1984, 1988, Krogh and Turek 1982). The ages by Turek et al. (1982, 1984) and Krogh and Turek (1982) were determined using the regressions devised by York (1966) and Davis (1982) respectively. Neither of these regressions has sufficiently accurate error estimation, and hence were recalculated using the regression and error treatment of Ludwig (1982b) as used in this study. The ages and associated errors are listed in Appendix A. The recalculation of these ages does not change the ages, but gives a better estimate of the errors, and matches the error treatment used here.

Mapping frequently cannot resolve significantly different ages. For example, in the Northern batholith, the Jostle Lake tonalite (2721 ± 4 Ma) and the Tee Lake tonalite (2673 ± 12 Ma) cannot be mapped as different in age since they occur in the same continuous granitoid terrain. Similarly, felsic volcanics, which typically occur as isolated volcanic centers, rarely show any age

Table 4. Revised and simplified table of lithologic units of the Mishibishu greenstone belt. Ages are from this study

SUPRACRUSTAL ROCKS		INTRUSIVE ROCKS	
		MAFIC AND FELSIC DIKES	
		GABBRO AND DIORITE PLUTONS	
		Iron Lake gabbro	2671±4 Ma
		GRANITOID BATHOLITHS - LATE	
METAVOLCANIC AND SUBVOLCANIC ROCKS		Tee Lake tonalite	2673±12 Ma
		Bowman Lake granite	2672 Ma
David Lakes pyroclastic breccia	2677±7 Ma	Mishibishu Lake stock	
		Central Pluton	
CLASTIC METASEDIMENTARY ROCKS			
CHEMICAL METASEDIMENTARY ROCKS			
FELSIC METAVOLCANIC ROCKS		GRANITOID BATHOLITHS - EARLY	
Chimney Point quartz-feldspar porphyry	2696±17 Ma	Southern Batholith	
		Pilot Harbour granite	2693±4 Ma
		Northern Batholith	
INTERMEDIATE METAVOLCANIC ROCKS		Jostle Lake tonalite	2721±4 Ma
MAFIC METAVOLCANIC ROCKS			

relations to each other.

Table 5 depicts six distinct events into which the ages may be categorized. These events were identified by Turek et al. (1984, 1988) as follows:

EVENT I	2888 Ma	volcanic and plutonic event - subcycle I volcanics
EVENT II	2743 Ma	volcanic and plutonic event - Cycle I volcanism
EVENT III	2717 Ma	volcanic and plutonic event - Cycle II volcanism
EVENT IV	2698 Ma	volcanic and plutonic cycle - Cycle III volcanism
EVENT V	2668 Ma	plutonic event
EVENT VI	2615 Ma	tectonic uplift

Events I through IV represent both plutonic and volcanic events. Events II, III, and IV represent lower, middle, and upper cycle Wawa volcanism respectively. Event V is a plutonic event during the Kenoran orogeny, and Event VI represents tectonic uplift in the Wawa and Gamitagama belts.

The ages of the Mishibishu belt are at the younger end of the scale. The oldest rock at 2721 ± 14 Ma is the Jostle Lake tonalite from the Northern Batholithic Complex, which falls into Event III. There appears to be only a single

Table 5. Summary of zircon ages for the Mishibishu, Michipicoten, and Gamitagama greenstone belts.

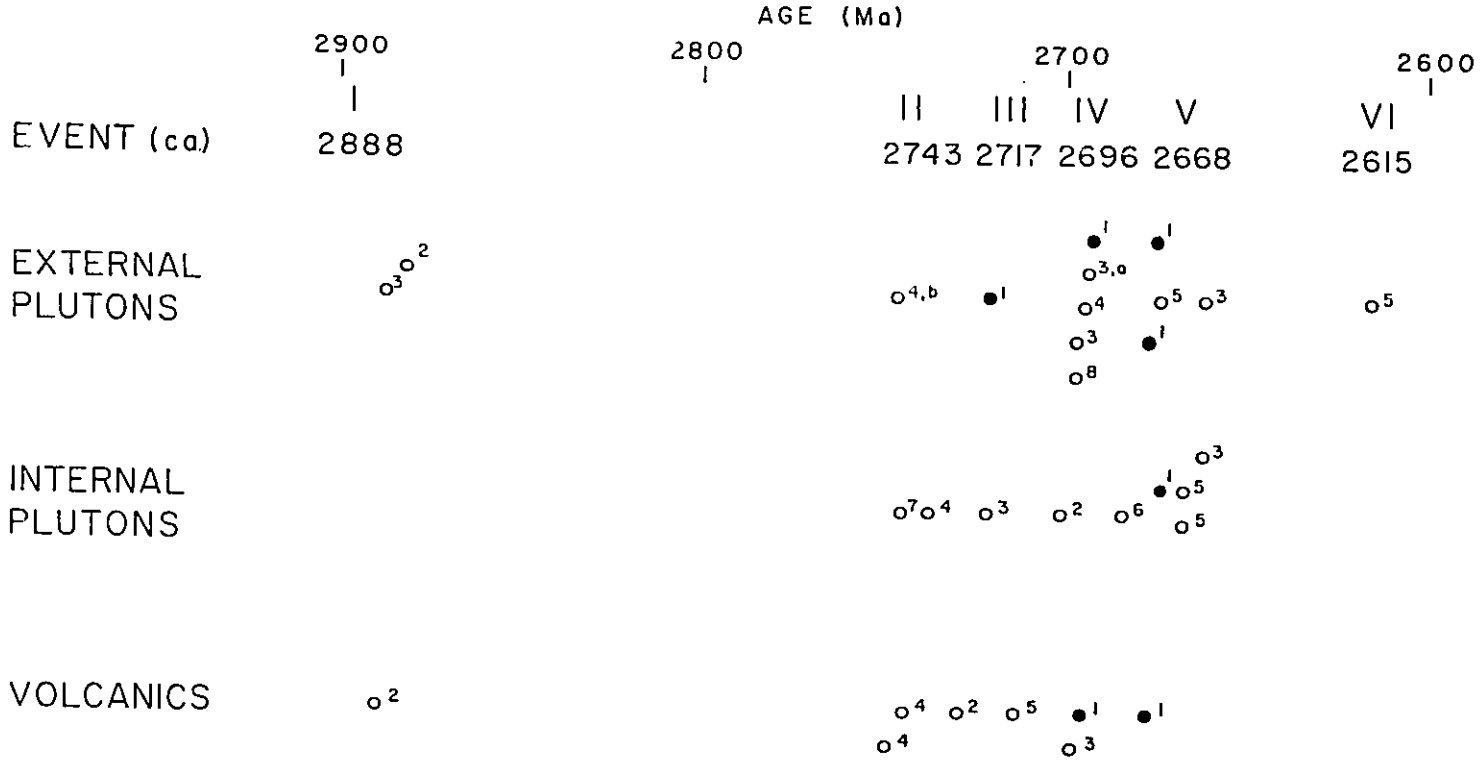

1. This study
2. Turek et al. 1988
3. Turek et al. 1984
4. Turek et al. 1982
5. Krogh and Turek 1982
6. Frarey and Krogh 1986
7. Sullivan et al. 1985
8. Corfu and Sage 1987

a cores dated at 2727 Ma

b cores indicate an older component greater than 2812 Ma

2696 ± 17 Ma, it fits into Event IV. The Pilot Harbour granite in the Southern batholith, with an age of 2693 ± 7 Ma also falls into Event IV. Event V (ca. 2670 Ma) was defined by plutonic episodes, and from this study, the Tee Lake tonalite of the Northern Batholithic Complex, the Bowman Lake granite, and the Iron Lake gabbro have similar ages of 2673 ± 12 Ma, 2672 Ma, and 2671 ± 2 Ma, respectively. The Iron Lake gabbro has an age identical to the Gamitagama gabbro at 2668 ± 2 Ma (Krogh and Turek 1982).

Plutonism defining Event V was thought to represent the Kenoran orogeny in this region, but widespread plutonic events of similar age appear in the Superior Province. Frarey and Korgh (1986) reported numerous granitic intrusions of this age across Ontario and Quebec, and Corfu and Grunsky (1985) reported similar ages for granitic plutons in the Batchawana greenstone belt, which is located nearly 200 km to the southeast of the Mishibishu area.

The David Lakes pyroclastic breccia has an age of 2677 ± 7 Ma and represents the youngest Archean volcanic event known at this time. Thus, Event V which was previously defined by plutonism alone, now must also include volcanism. Since the mapping by Reid and Reilly (1987) and Reid et al. (1989) did not show any associated mafic volcanism, this younger pyroclastic is not considered to be part of a volcanic cycle, but must represent an isolated episode of

felsic volcanism. The ages for the Wawa and Gamitagama belts are shown in Table 5 and listed in Appendix A.

CHAPTER VIII

CONCLUSIONS

The evolution of the Mishibishu greenstone belt occurred over a time span of at least 50 Ma, between 2721 Ma and 2671 Ma. This does not preclude the existence of older rocks, however. The Mishibishu belt is believed to be an extension of the Wawa and Gamitagama greenstone belts, based on their comparable lithology and age of volcanism, which relates to the upper-cycle volcanism in the Wawa belt (2696 Ma).

The association of volcanism and plutonism identified in the Wawa and Gamitagama belts is further confirmed by similar events in the Mishibishu belt. A volcano-plutonic event occurred ca. 2670 Ma ago, and this is the first such age for an Archean volcanic rock. This volcanism matches the well-documented plutonic event in the Superior Province at about 2670 Ma. This extensive plutonic event is both felsic and mafic, since the Iron Lake gabbro falls into this time slot. This clearly indicates that volcanism and plutonism in the evolution of a greenstone belt and associated granitic terrains, which are characteristic of the Archean; tend to be coeval, and some episodes may very well be cogenetic.

APPENDICES

APPENDIX A

Recalculated Ages

The published ages for the Michipicoten, Gamitagama, and Abitibi greenstone belts referred to in this study, were not calculated using the regression and error treatment of Ludwig (1982b). The following table provides both the original published ages and recalculated ages using the Ludwig (1982b) regression. The ages for the Michipicoten area by Turek et al. (1988) did not require recalculation but are included here because of their importance to this study. All the recalculated ages are given with 2-sigma errors.

Recalculated ages (based on Ludwig 1982b) for the Michipicoten and Gamitagama greenstone belts.

Sample No.	Published Concordia Age (Ma)		Recalculated Concordia Age (Ma)		Remarks
	Upper Intercept	Lower Intercept	Upper Intercept	Lower Intercept	
Michipicoten belt (Turek et al. 1982)					
641	2696±2	385±30	2696±4	382±52	Model 2 p=4%
636	2744±10	364±126	2644±19	358±258	Model 2 p=0%
659	2749±2	107±19	2749±3	105±35	Model 2 p=16%
664	2737±6	345±19	2739±13	355±51	Model 2 p=0%
646	2747±6	453±14	2746±9	460±24	Model 2 p=10%
	2812±3	573±8	-	-	older component age
Michipicoten belt (Turek et al. 1984)					
671	2698±11	388±130	2697±21	374+273	Model 2 p=11%
672	2723±1	293±10	2723±19	292±187	Model 1 p=91%
676	2662±5	254±52	2663±24	255±259	Model 1 p=69%
678	2694±3	312±62	2695±10	284±172	Model 2 p=0%
674	2698±1	408±44	2699±3	414±108	Model 2 p=9%
670	2888±2	445±35	[illegible]	443±72	Model 2 p=21%

Sample No.	Published Concordia Age (Ma)		Recalculated Concordia Age (Ma)		Remarks
	Upper Intercept	Lower Intercept	Upper Intercept	Lower Intercept	
Gamitagama belt (Krogh and Turek 1982)					
516	$2713\pm^{3}_{2}$	461	2713±4	471±335	Model 1 p=94%
504	$2668\pm^{2}_{2}$	370	2668±3	372±59	Model 1 p=70%
Tk-78-1	$2668\pm^{2}_{2}$	371	2668±3	374±75	Model 1 p=64%
511	$2615\pm^{9}_{8}$	634	2615±9	635±34	Model 2 p=21%
Abitibi belt (Frarey and Krogh 1986)					
FC-9-76	$2685\pm^{3}_{3}$	495	2684±4	495±31	Model 1 p=33%
Michipicoten belt (Sullivan et al. 1985)					
Jubilee Stock	2745±3	300	2745±6	330±179	Model 2 p=15%
Michipicoten belt (Turek et al. 1988)					
695	2889±9	-	-	-	Model 1 p=78%
696	2881±4	-	-	-	Model 1 p=45%
679	2702±30	-	-	-	Model 2 p=1%
598	2729±3	-	-	-	Model 2 p=25%

APPENDIX B

U-Pb Chemistry

Laboratory procedures are provided for zircon cleaning, dissolution and separation of U and Pb. Cleaning of the crystals is necessary to remove common Pb contamination. U and Pb are separated using ion exchange columns.

To obtain an age for a rock, three mass spectrometer runs are required. These include U and Pb isotope dilution (ID) and Pb isotope composition (IC) analyses. The U ID run allows the concentration of U in the sample to be determined. The Pb IC and ID runs are used to calculate the isotopic concentrations of Pb in the sample. For details regarding these calculations, refer to Faure (1986) and Ludwig (1982a).

APPENDIX B

U-Pb Chemistry

Zircon Wash Procedure

1. Put zircons into clean 30 mL glass beaker. Use ultrapure H_2O to wash zircons out of petri dish if necessary.
2. Add approximately 10 mL of 7N HNO_3.
3. Put beaker on hot plate and heat at low temperature for 1 hour. Use a timer.
4. Ultrasound for at least 1 hour in HNO_3.
5. Decant supernatant.
6. Rinse zircons with ultrapure H_2O
7. Add 10 mL of ultrapure H_2O and heat gently for a half hour, without boiling.
8. Ultrasound for 1 hour.
9. Repeat steps 5 through at least 3 times.
10. Collect the zircons on an acetate or teflon filter paper and store in a covered petri dish until ready for weighing and dissolution.

APPENDIX B - continued

Dissolution of Zircons

1. Weigh out 1 to 2 mg of the cleaned zircons into a teflon bomb and add 0.5 mL HF and 2 drops 7N HNO_3.
2. Put bombs in oven at 195°C for a minimum of 5 days.
3. Cool bombs to room temperature and open.
4. Dry slowly on hot plate (about 1 hour). Seal cap in parafilm and set aside.
5. When dry, add 2 drops of ultrapure HNO_3. Evaporate to dryness, then add 0.5 mL 6N HCℓ.
6. Reassemble bombs and place in oven at 195° overnight (minimum 4 hours).
7. Remove bombs from oven and cool.
8. Quantitatively transfer to a 5 mL teflon beaker.
9. Quantitatively transfer ca. 2mL of solution in step (8) to a 5 mL teflon beaker and an appropriate amount of the mixed U-Pb tracer.
10. Evaporate to dryness. Ready for U-Pb separation techniques.

APPENDIX B - continued

HCℓ Technique for IC's

1. Add 1 mL 1N HCℓ to sample beakers. Allow time for residue to dissolve.
2. Rinse teflon columns in deionized water several times and mount on racks.
3. Load columns with 0.5 mL cleaned anion resin in 5N HCℓ. Allow liquid to drain.
4. Flush columns with 2 mL of 5N HCℓ.
5. Label 5 mL teflon beakers for Pb IC's (unspiked).
6. Condition columns with 2 mL 1N HCℓ.
7. Load the dissolved residue onto the columns.
8. Wash with 1 mL 1N HCℓ.
9. Wash again with 1 mL 1N HCℓ.
10. Place 5 mL teflon beakers under columns.
11. Elute Pb with 3 mL 5N HCℓ.
12. Add 1 drop 1/4 N H_3PO_4 to beaker. (optional).
13. Evaporate to dryness and store sealed in parafilm.

APPENDIX B - continued

HCℓ Technique for ID's

1. Add 1 mL 3N HCℓ to sample beakers. Allow time for residue to dissolve.
2. Rinse columns in deionized water several times and mount on racks.
3. Load columns with 0.5 mL of cleaned anion resin in 5N HCℓ. Let liquid drain.
4. Flush columns with 2 mL 5N HCℓ.
5. Label 5 mL teflon beakers for ID's (spiked).
6. Condition columns with 2 mL 3N HCℓ.
7. Load the dissolved residue onto the columns.
8. Wash with 1 mL 3N HCℓ.
9. Wash again with 1 mL 3N HCℓ.
10. Place 5 mL teflon beakers under columns.
11. Elute Pb with 2 mL 5N HCℓ.
12. Elute U with 2 mL deionized water.
13. Add 1 drop 1/4 N H_3PO_4 to beakers. (optional)
14. Evaporate to dryness and store sealed in parafilm.

APPENDIX C

Petrographic Descriptions

Petrographic Descriptions

G4 David Lakes pyroclastic

Light grey, foliated, brecciated pyroclastic rock of rhyolitic composition with clasts to 4 cm. The mineralogy of the rock is 35% quartz, 20% plagioclase, 10% K-feldspar, 15% carbonate, 10% sericite, 5% chlorite, and 5% sphene and pyrite. Quartz is recrystallized; plagioclase and K-feldspar crystals are euhedral to subhedral; sericite in matrix defines foliation.

G14 Tee Lake tonalite

Grey and white, phaneritic, medium-grained, slightly foliated with 20% quartz, 45% plagioclase, 15% K-feldspar, 5% biotite, and a total of 18% of epidote, chlorite, and sphene. Polygonal recrystallized quartz; plagioclase shows sausseritization; biotite defines weak foliation.

G15 Jostle Lake tonalite

Pink and grey-green, weakly foliated, phaneritic, medium-grained, composed of 25% quartz, 65% plagioclase, 10% hornblende and a trace of K-feldspar. Elongated hornblende defines foliation.

G16 Iron Lake gabbro

Medium-grained, dark grey-green, weakly foliated and

magnetic consisting of 4% quartz, 45% plagioclase, 5% K-feldspar, 8% biotite, 15% pyroxene, 20% hornblende, and 3% opaques. Minor interstitial quartz oscillatory zoning in plagioclase; pyroxene is replaced by hornblende.

G17 **Bowman Lake granite**

Coarse-grained, pink and white with phenocrysts up to 5 cm., consisting of 25% quartz, 15% K-feldspar, 55% plagioclase, 2% biotite, 1 to 2% clinozoisite and minor sericite and zircon. Oscillatory zoning, deformed twins in plagioclase; polygonal recrystallized quartz; biotite defines weak foliation.

G22 **Pilot Harbour granite**

Medium- to coarse-grained, light grey-white with phenocrysts up to 3 cm. Composed of 25% quartz, 45% plagioclase, 15% K-feldspar, 5% hornblende, 2% biotite, 2% epidote, 2% chlorite, 4% sericite, and minor sphene and zircon. Oscillatory zoning, deformed twins, sausseritization in plagioclase; polygonal recrystallized quarts.

G25 **Chimney Point porphyry**

Medium-grained, weakly foliated, dark grey with red-brown staining and of andesitic composition. In thin section, the rock is quartz-feldspar porphyry and

contains 30% quartz, 25% plagioclase, 30% sericite, 10% chlorite, 5% carbonate, minor opaques. Plagioclase is extensively altered to sericite, twin lamellae are deformed, and oscillatory zoning is evident; polygonal quartz occurs as phenocrysts with plagioclase, and in matrix with sericite and chlorite; extensive carbonitization (brown staining) prominent in hand specimen; sericite and chlorite in matrix define weak foliation; carbonate occurs in veinlets with quartz and sericite.

Photomicrographs in plain polarized light of zircons from the Mishibishu greenstone belt.

Plate 1. G4, - 100 + 200 mesh, M1°. David Lakes felsic pyroclastic breccia. Four clear, euhedral crystals, with few inclusions. Typical volcanic zircons.

Plate 2. G14, - 100 + 200 mesh, M0°. Tee Lake tonalite from the Northern Batholithic Complex. Four clear, subhedral crystals and one with euhedral terminations.

Plate 3. G15, - 100 + 200 mesh, NM0°. Jostle Lake tonalite from the Northern Batholithic Complex. Three clear, subhedral crystals, with minor inclusions and fractures.

Plate 4. G16, - 100 + 200 mesh, M0°. Iron Lake gabbro. Two subhedral zircons are transluscent and fractured.

Plate 5. G17, - 100 + 200 mesh, M3°. Bowman Lake granite. Two subhedral zircons are shown; one is opaque, the other transluscent. Both crystals are extensively fractured.

Plate 6. G22, - 100 + 200 mesh, NM0°. Pilot Harbour granite from the Southern Batholith. Four crystals shown are clear, transparent and free from inclusions.

Plate 7. G25, - 100 + 200 mesh, NM0°. Chimney Point porphyry. Single transluscent crystal. Fractures and inclusions are apparent.

Plate 8. G25, - 100 + 200 mesh, NM0°. Chimney Point porphyry. Single crystal containing what is interpreted to be a xenocrystic core.

Plate 1.

Plate 2.

Plate 3.

Plate 4.

Plate 5.

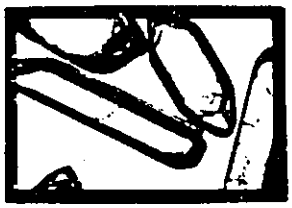

Plate 6.

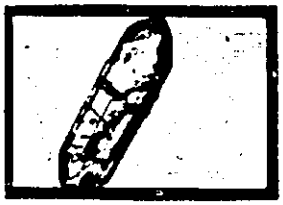

Plate 7.

Plate 8.

0 0.1 mm

APPENDIX D

Sample Locations

Sample Locations

	Sample	Latitude	Longitude
G4	David Lakes pyroclastic breccia	48°02'38"N	85°40'26"W
G14	Tee Lake tonalite	48°06'57"N	85°41'26"W
G15	Jostle Lake tonalite	48°05'34"N	85°12'24"W
G16	Iron Lake gabbro	48°08'29"N	85°34'29"W
G17	Bowman Lake granite	47°59'08"N	85°21'28"W
G22	Pilot Harbour granite	47°55'15"N	85°37'30"W
G25	Chimney Point porphyry	47°58'55"N	85°52'12"W

REFERENCES

Acton, F.S. 1959. Analysis of straight-line data. John Wiley and Sons.

Bass, M.N. 1961. Regional tectonics of part of the Southern Canadian Shield. Journal of Geology, v. 69, pp. 668-702.

Bell, J.M. 1905. Iron ranges of Michipicoten West. In Ontario Bureau of Mines, 14, part 1, 374 pp.

Bennett, G. and Thurston, P.C. 1977. Geology of the Pukaskwa River-University River Area, Districts of Algoma and Thunder Bay. Ontario Division of Mines, Geoscience Report 153, 60 pp.

Bowen, R.P. 1986. Mishibishu Lake area, Districts of Algoma and Thunder Bay. In Summary of Field Work and Other Activities 1986. Ontario Geological Survey Miscellaneous Paper 132, pp. 107-110.

Bowen, R.P., and Logothetis, J. 1985. Mishibishu Lake area, Districts of Algoma and Thunder Bay. In Summary of Field Work and Other Activities 1985. Ontario Geological Survey Miscellaneous Paper 126, pp. 78-82.

Brooks, C., Hart, S.R., and Wendt, I. 1972. Realistic use of two-error regression treatments as applied to rubidium-strontium data. Review of Geophysics and Space Physics, 10, pp. 551-577.

Coleman, A.P. 1899. Copper regions of the upper lakes. Ontario Bureau of Mines, 8, part 2, pp. 121-174.

Coleman, A.P., and Willmott, A.B. 1899. Michipicoten Iron ranges. Ontario Bureau of Mines, 8, part 2, pp. 254-258.

Collins, W.H. and Quirke, T.T. 1926. Michipicoten Iron Ranges, part 1. In Michipicoten Iron Ranges, Geological Survey of Canada, Memoir 147, 175 pp.

Corfu, F. and Grunsky, E.C. 1987. Igneous and tectonic evolution of the Batchawana greenstone belt, Superior Province: a U-Pb zircon and titanite study. Journal of Geology, 95, pp. 87-105.

Corfu, F. and Sage, R.P. 1987. A precise U-Pb zircon age for a trondhjemite clast in the Dore conglomerate, Wawa, Ontario. Institute on Lake Superior Geology, Proceedings and Abstracts, 33, 1, p. 19.

Cummings, G.L. 1969. A recalculation of the age of the solar system. Canadian Journal of Earth Sciences, 4, pp. 719-735.

Cummings, G.L., Rollett, J.S., Rosotti, F.J.C., and Whewell, R.J. 1972. Statistical methods for the computation of stability constants, I. Straight-line fitting of points with correlated errors. Journal of Chemical Society, Dalton Trans., pp. 2652-2658.

Davis, D.W. 1982. Optimum linear regression and error estimation applied to U-Pb data. Canadian Journal of Earth Sciences, 19, pp. 2142-2149.

Doe, B.R. 1970. Lead Isotopes. Springer-Verlag, New York, 137 pp.

Evans, E.L. 1940. Geology of the Mishibishu Lake area. Ontario Department of Mines, 49, part 9, 14 pp.

Faure, G. 1986. Principles of isotope geology, second edition. John Wiley and Sons, 589 pp.

Frarey, M.J. and Krogh, T.E. 1986. U-Pb zircon ages of late internal plutons of the Abitibi and eastern Wawa subprovinces, Ontario and Quebec. In Current Research, Part A, Geological Survey of Canada, Paper 86-1A, pp. 43-48.

Goldich, S.S., and Mudrey, M.G. 1972. Dilatancy model for discordant U-Pb zircon ages. In Contributions to Recent Geochemistry and Analytical Chemistry (A.P. Vinogradov volume), A.I. Tugarinos, ed., Moscow, Nauka Publ. Office, pp. 415-418.

Goodwin, A.M. 1954. Geology of townships 31 and 32, range 26. Private unpublished report prepared for Algoma Ore Properties, Limited. Regional Geologist's Files, Ontario Ministry of Natural Resources, Sault Ste. Marie, Geology, 1954.

Goodwin, A.M. 1962. Structure, stratigraphy, and origin of iron formations, Michipicoten area, Algoma District, Ontario, Canada. Geological Society of America Bulletin, 73, No. 5, pp. 561-586.

Heather, K.B. 1985. Gold showings of the Mishibishu Lake area, Thunder Bay District. In Summary of Field Work and Other Activities 1985, Ontario Geological Survey Miscellaneous Paper 126, pp. 83-89.

Heather, K.B. 1986. Mineralization of the Mishibishu Lake greenstone belt. In Summary of Field Work and Other Activities 1987. Ontario Geological Survey Miscellaneous Paper 132, pp. 283-291.

Krogh, T.E. 1973. A low contamination method for hydrothermal decomposition of zircon and extraction of U and Pb for isotopic age determinations. Geochimica et Cosmochimica Acta, 37, pp. 485-494.

Krogh, T.E. 1982. Improved accuracy of U-Pb zircon ages by the creation of more concordant systems using an air abrasion technique. Geochimica et Cosmochimica Acta, 46, pp. 637-649.

Krogh, T.E. and Turek, A. 1982. Precise U-Pb zircon ages from the Gamitagama greenstone belt, southern Superior Province. Canadian Journal of Earth Sciences, 19, pp. 859-867.

Ludwig, K.R. 1980. Calculation of uncertainties of U-Pb isotopic age data. Earth and Planetary Science Letters, 46, pp. 212-220.

Ludwig, 1982a. A computer program to convert raw Pb-U-Th isotope ratios to blank-corrected isotope ratios and concentrations, with associated errors and error-correlations. United States Geological Survey, Open-file Report 82-820, 15 p.

Ludwig, 1982b. Programs for filing and plotting U-Pb isotope data for concordia diagrams, using an HP-9830 computer and HP-9862 plotter. United States Geological Survey, Open-file Report 82-386, 22 p.

Mattison, J.M. 1972. Preparation of hydrofluoric, hydrochloric, and nitric acids at ultralow lead levels. Analytical Chemistry, 44, pp. 1715-1716.

McIntyre, G.A., Brooks, C., Compston, W., and Turek, A. 1966. The statistical assessment of Rb-Sr isochrons. Journal of Geophysical Research, 71, pp. 5459-5468.

Reid, R.G., and Reilly, B.A. 1987. Mishibishu Lake area, Districts of Algoma and Thunder Bay. In Summary of Field Work and Other Activities 1987. Ontario Geological Survey Miscellaneous Paper 137, pp. 138-145.

Reid, R.G., Bowen, R.P., Reilly, B.A., Logothetis, J., and Heather, K.B., 1989. Geology, structure, and mineralization of the Mishibishu Lake area, Districts of Algoma and Thunder Bay. Ontario Geological Survey, Open-file Report. (In press).

Stacey, J.S., and Kramers, J.D. 1975. Approximation of terrestrial lead isotope evolution by a two-stage model. Earth and Planetary Science Letters, 26, pp. 207-221.

Steiger, R.H., and Jäger, E. 1977. Subcomission on Geochronology: Convention on the use of decay constants in geo- and cosmochronology. Earth and Planetary Science Letters, 28, pp. 359-362.

Sullivan, R.W., Sage, R.P., and Card, K.D. 1985. U-Pb zircon age of the Jubilee stock in the Michipicoten greenstone belt near Wawa, Ontario. In Current Research, Part B, Geological Survey of Canada, Paper 85-18, pp. 361-365.

Tilton, G.R. 1960. Volume diffusion as a mechanism for discordant lead ages. Journal of Geophysical Research, 65, 9, pp. 2933-2945.

Turek, A., Smith, P.E., and Van Schmus, W.R. 1982. Rb-Sr and U-Pb ages of volcanism and granite emplacement in the Michipicoten belt-Wawa, Ontario. Canadian Journal of Earth Sciences, 19, pp. 1608-1626.

Turek, A., Smith, P.E., and Van Schmus, W.R. 1984. U-Pb zircon ages and the evolution of the Michipicoten plutonic volcanic terrane of the Superior Province, Ontario. Canadian Journal of Earth Sciences, 21, pp. 457-464.

Turek, A., Van Schmus, W.R., and Sage, R.P. 1988. Extended volcanism in the Michipicoten greenstone belt, Wawa, Ontario. Geological Association of Canada and Mineralogical Association of Canada, Program with Abstracts, 13, p. 127.

Wetherill, G.W. 1956. Discordant uranium-lead ages. Trnas. American Geophys. Union, 37, pp. 320-326.

Wetherill, G.W. 1963. Discordant uranium-lead ages - Part 2: Discordant ages resulting from diffusion of lead and uranium. Journal of Geophysical Research, 68, pp. 2957-2965.

Wolfe, W.J. 1976. Regional geochemical reconnaissance of Archean metavolcanic-metasedimentary belts in the Pukaskwa region. Ontario Division of Mines, Geoscience Report 158, 54 pp.

York, D. 1966. Least-squares fitting of a straight line. Canadian Journal of Physics, 44, pp. 1079-1086.

York, D. 1969. Least-squares fitting of a straight line with correlated errors. Earth and Planetary Science Letters, 5, pp. 320-324.

Vita Auctoris

BORN: December 2, 1955, Leamington, Ontario, Canada

SECONDARY SCHOOL

Kingsville District High School, Kingsville, Ontario Canada. 1974.

POST-SECONDARY EDUCATION

Control Data Institute, Willowdale, Ontario, Canada. 1975.

Ryerson Polytechnical Institute, Toronto, Ontario, Canada. 1983.

University of Windsor, Windsor, Ontario, Canada, B.Sc., 1987.

PUBLICATIONS

Turek, A., Keller, R., and Van Schmus, W.R. 1989. U-Pb ages for the Mishibishu greenstone belt near Wawa, Ontario. Geological Association of Canada and Mineralogical Association of Canada, Program with Abstracts, 14, p. A55.

Turek, A., Keller, R., Weber, W., and Van Schmus, W.R. 1987. New U-Pb zircon ages for the Rice Lake greenstone belt, southeastern Manitoba. Geological Association of Canada and Mineralogical Association of Canada, Program with Abstracts, 12, p. 97.

Turek, A., Keller, R., Van Schmus, W.R., and Weber, W. 1989. U-Pb zircon ages for the Rice Lake area, southeastern Manitoba. Canadian Journal of Earth Sciences, 26, pp. 23-30.